REVIEW

Check for updates

Receptor or rhetoric? a critical review of glucose transporter-targeting in nanomedicine

Matthew Zammit, [*ab] Jason Fleming [ab] and Martin Volk [c]

Despite the significant promise shown by nanoparticle-based diagnostics and therapies, there remain considerable challenges, especially concerning their targeting accuracy and specificity. This critical review explores glucose-conjugated nanoparticles (NPs) as more selective diagnostic and therapeutic tools for cancer treatment and drug transfer across the blood–brain barrier, with a particular focus on their interactions with glucose transporters (GLUTs) that are typically overexpressed in cancer and brain capillary endothelial cells. Although there are many reports of increased NP uptake upon glucose-functionalisation, the mechanistic basis for this targeting remains unclear. Here, we systematically evaluate the literature across inorganic, polymeric, liposomal, and micellar NP systems, examining how the nature of the linker and the conjugation strategy influence targeting. We place particular emphasis on the question whether convincing evidence for GLUT-mediated NP uptake has been provided, which is only possible using rigorous competition or inhibition control studies. We demonstrate that there is no such evidence for studies using direct conjugation of glucose, or conjugation *via* a short linker, to a solid NP. This is consistent with structural models placing the glucose-binding site deep within the transporter. However, conjugation at the end of sufficiently long and flexible linkers can enable genuine GLUT targeting. Similarly, the position and chemical nature of the glucose conjugation site needs to be considered carefully. Taken together, our review identifies a set of design principles that provide a rational foundation for future nanomedicine development. Studies incorporating these principles with stringent GLUT controls are more likely to generate transporter-specific platforms with genuine translational potential.

Matthew Zammit is an ENT registrar in the North West of England and a PhD candidate in Surgery & Oncology at the University of Liverpool. He previously completed an MPhil in Cancer Medicine investigating glycoconjugation strategies for gold nanoparticles using PEGylated linkers to enhance tumour targeting in oropharyngeal squamous cell carcinoma. His current research focuses on nanoparticle-guided fluorescence imaging and the

Matthew Zammit

translational evaluation of tumour-specific probes for surgical margin delineation during transoral robotic surgery. His academic interests centre on the clinical translation of nanotechnology-driven imaging platforms in head and neck oncology.

Mr Jason Charles Fleming is Reader in Head and Neck Oncology at the University of Liverpool and Honorary Consultant Otolaryngologist and Head & Neck Surgeon at Liverpool University Hospitals NHS Foundation Trust. His research focuses on the evaluation and development of novel surgical technologies for oncology applications. He is Co-Chief Investigator of the international PROTIS randomised controlled trial investigating proton beam therapy

Jason Fleming

in sinonasal cancer. Clinically, he leads robotic head and neck surgery at Liverpool and was the first surgeon in Europe accredited to perform transoral robotic surgery using the da Vinci SP platform.

4874 | *J. Mater. Chem. B*, 2026, **14**, 4874–4902

This journal is © The Royal Society of Chemistry 2026

1. Introduction

Despite therapeutic advances in oncology, cancer remains a formidable medical challenge. The morbidity of non-personalised treatment strategies including chemoradiotherapy adds another complexity for patients, although newer immunotherapy approaches are demonstrating the benefit of a more tumour-specific approach. An ability to target cancer cells from normal bystander tissue with high accuracy remains the holy grail for cancer treatment delivery to maximise therapeutic benefit and minimise toxicity.

Although nanomedicine, the use of nanoparticles (NPs) for diagnosis and therapy, faces its own challenges, it holds great promise for cancer treatment, even though its translation into clinical settings has so far been limited.[1–7] Some NPs have properties which make them directly suitable for diagnostic or imaging purposes, such as the intrinsic fluorescence of quantum dots (QDs)[8] or the contrast enhancement in computed tomography imaging by gold nanoparticles (AuNPs).[9] Therapeutically, AuNPs have been explored as photothermal and photodynamic agents[10] or radiation sensitizers.[11] However, their utility is greatly enhanced when drug molecules or other functional ligands with diagnostic or therapeutic properties are attached to the surface or incorporated into porous inorganic, liposomal, micellar, or polymeric NPs.[12–18] Since NPs can be easily functionalised with multiple ligands simultaneously, it is possible to combine their intrinsic properties with those of its ligands, creating platforms with multi-functional diagnostic and/or therapeutic capabilities.[19]

Moreover, these functionalities may even be directed towards specific cell types, such as cancer cells, by the addition of ligands that promote specific cell selection and targeted active agent delivery.[20–26] Thus, the ease with which NPs may be multi-functionalised to include targeting as well as diagnostic and/or therapeutic capabilities may prove to be the route to realise their true potential. NPs are widely believed to undergo passive targeting towards cancer tissue due to its leaky vasculature and poor lymphatic drainage, the so-called 'enhanced permeability and retention' (EPR) effect;[22,27] this is often cited as one of the main advantages of nanomedicines compared to small molecules. However, the EPR effect shows only limited discrimination between cancerous and healthy tissue[28] and its applicability for "real-life" treatment has been questioned.[23,29,30] Moreover, it is not of help for the treatment of ill-defined or micro-metastatic tumours, haematological malignancies or residual cancer cells in a post-surgical tumour bed. Therefore, active targeting strategies which direct NPs specifically to cancer cells once they have reached the target tissue are of great interest and there is even potential to define ligand targeting to specific intracellular organelles.[31]

Active targeting of NPs towards cancer cells has been attempted using a wide variety of ligands, including monoclonal antibodies, proteins (e.g. transferrin) and peptides, aptamers, folates and various carbohydrates.[20–22] In this review, we focus on the use of glucose as the targeting ligand, as it is readily conjugated to larger molecules or NPs through multiple synthetic approaches.

The concept of tumour-enhanced glucose uptake was first described in 1927 by Otto Warburg and has been extensively studied since.[32] It is well established that cancer cells often make use of aerobic glycolysis for deriving their energy instead of the more efficient, albeit slower, mitochondrial metabolization of glucose; this provides a carbon source for the synthesis of essential biomolecules needed for rapid cell division, but may also confer other advantages to the cancer cell such as acidification of the environment.[33] The Warburg effect is the basis for new approaches in the treatment of cancer, including inhibiting the glycolytic pathway to selectively stunt the growth of cancer cells,[34] and improving tumour imaging using positron emission tomography after application of ^{18}F-fluorodeoxyglucose (^{18}F-FDG), which accumulates in cells with high glycolytic activity and is a common clinical imaging modality in clinical practice.[35,36]

Glucose transporters (GLUTs) are overexpressed on the plasma membrane of many cancer cell types, reflecting this altered metabolic profile.[37–39] GLUTs are a family of transmembrane proteins that facilitate the diffusion of glucose through the plasma membrane.[7,37,38] Owing to the brain's high energy demands, GLUTs are also abundantly expressed in brain capillary endothelial cells (BCECs); as a result, GLUT-mediated transcytosis has been proposed as a mechanism for delivering NPs across the blood–brain barrier (BBB) to support diagnosis, imaging and treatment of brain tumours.[40–43] Additionally, GLUT targeting has been proposed for antigen delivery to dendritic cells, which overexpress GLUTs, for cancer immunotherapy strategies.[44]

The overexpression of GLUTs has been exploited for targeted delivery of glycoconjugated anticancer drugs, with the goal of reducing required dosages and minimizing side effects.[39,45–48] Similarly, many different approaches to target cancer cells or facilitate BBB transcytosis using glucose-functionalised NPs have been described in the literature. In this review, we critically assess these methods, specifically examining whether the reported enhanced uptake of glucose-conjugated NPs can be attributed to interactions with GLUTs or are a result of non-

Martin Volk obtained a degree in Physics (1986) and a PhD from the Technical University of Munich (1991). After post-doctoral work in Munich and at the University of Philadelphia, undertaking nano-second- and femtosecond time-resolved spectroscopic studies on a wide range of biological and chemical systems, he took up a position at the University of Liverpool in 1999. His current research interests focus on fast processes of protein folding as well as research on gold nanoparticles, such the structure and dissociation dynamics of peptide capping layers and the application of gold nanoparticles in photodynamic therapy.

Martin Volk

This journal is © The Royal Society of Chemistry 2026

J. Mater. Chem. B, 2026, **14**, 4874–4902 | **4875**

specific binding to the plasma membrane. The latter mechanism would undermine the principle of selective targeting. We highlight reports of the successful implementation of GLUT targeting. However, for many of the proposed glycoconjugation methods this has not been shown conclusively, and we will discuss in detail why in many of these cases interaction of the glycoconjugated NP with GLUTs is in fact unlikely.

2. Background

2.1. The target: glucose transporters

GLUTs, which facilitate glucose diffusion across the plasma membrane, belong to the solute carrier gene family 2A (SLC2A), a sub-group of the major facilitator superfamily (MFS) of proteins.[49] There are 14 GLUT isoforms, which are grouped into three classes. The class I GLUTs, comprising GLUT1,2,3,4 and 14 (a gene duplicate of GLUT3), exhibit high glucose binding selectivity and are over-expressed in many cancer types,[7,37,38] as well as BCECs.[24,40]

The glucose transport mechanism of class I GLUTs has been described in detail recently,[49,50] after the structures of several GLUTs were determined.[51–53] Like most MFS proteins, GLUTs adopt a canonical fold consisting of 12 transmembrane (TM) helices linked by extra- and intracellular loops or short helices. These TM helices form two helical bundles with pseudo-2-fold symmetry, enclosing a central cavity which constitutes the major substrate binding site. The two helical bundles can adopt two major conformations, namely outward-facing, where the central binding site is accessible from the cell exterior (Fig. 1), or inward-facing, where the binding site is open to the cytosol. Under physiological conditions with high extracellular and low intracellular glucose concentrations, glucose binds to the central binding site in the outward-facing conformation. The helix bundles then undergo a rocker-switch structural rearrangement to form the inward-facing conformation, from which glucose can be released to the low-concentration environment of the cytosol, thereby facilitating the concentration-driven transport of glucose across the plasma membrane.

GLUT1 is the most widely expressed isoform and the most commonly over-expressed GLUT in cancer cells. Its structure has been determined in detail,[51,53] but only in the inward-open conformation, the state that facilitates glucose release into the cytosol. More relevant for targeting of overexpressed GLUT transporters by glucose conjugated NPs is the outward-open conformation, i.e. the conformation in which the binding site is accessible from the extracellular fluid, which also is the preferred GLUT conformation in absence of substrate.[54,55] The only GLUT for which an outward-open structure has been determined experimentally is GLUT3,[52] as shown in Fig. 1. However, class 1 GLUTs are generally accepted to have highly conserved structures; for example, the inward-facing structures of GLUT1 and GLUT4, which have 66% sequence identity and 87% similarity based on pairwise sequence alignment using the Smith-Waterman algorithm on the Protein Information Resource,[56] are superimposable with root-mean-square deviation (RMSD) values of 1.09–1.13 Å.[57] GLUT3 has 66% sequence identity and 88% similarity with GLUT1, strongly suggesting that the outward-facing conformations of GLUT1 and GLUT4 strongly resemble that of GLUT3. This is further supported by molecular dynamics (MD) simulations[58] and the observation that the glucose binding site of the outward-open GLUT3 is very similar to that of the inward-open conformation of GLUT1.[52]

Fig. 1 shows the structure of GLUT3 in the outward-open conformation, with the main glucose binding site indicated in colour. The top view (right) reveals a narrow channel with a
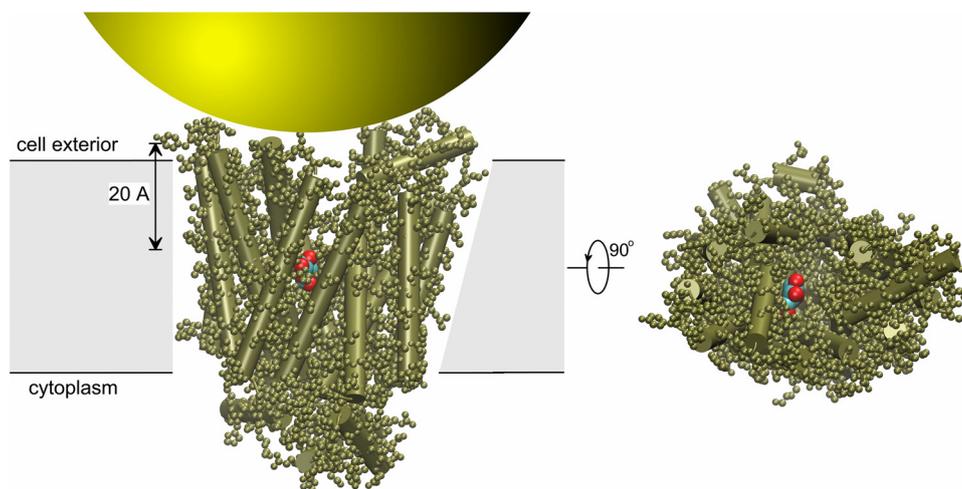

Fig. 1 Structure of GLUT3 in the outward-open conformation (PDB-id 4ZWC).[52] The protein is shown in tan colour in CPK representation, with α-helices indicated as cylinders. The lower glucose ring of the maltose ligand present in this structure is rendered in van der Waals (VDW) format (oxygen red, carbon cyan) as an indication of the glucose binding site; in the maltose-bound outward-occluded conformation this ring overlaps perfectly with glucose in the glucose-bound GLUT3 outward-occluded conformation and thus can be taken as a good indication of the location of glucose in the outward-open conformation.[52] Left: side-view, with the plasma membrane indicated schematically in grey; right: view from the top (i.e. from the exofacial side of the membrane). Also shown is part of a NP with 10 nm diameter (to scale). This image was made using VMD software.[60]

diameter of 4–5 Å[52,59] leading from the extracellular space to the binding site. The top of the glucose molecule, when bound in this site, lies approximately 20 Å from the residues lining the channel entrance.

Molecular docking and molecular dynamics (MD) simulations provide complementary insights to experimental GLUT structures.[55,58,59,61–63] In these simulations, the outward-facing conformations were derived either from (i) the experimental structure of GLUT3, (ii) homology models of GLUT1 based on the structure of xylose permease from *Escherichia coli*, a close bacterial homologue, or (iii) MD simulations starting with the inward-open conformation of GLUT1. While the specific findings vary, the studies consistently identify the main glucose binding site in the central cavity of the protein, as shown in Fig. 1. Additionally, they propose the presence of transient binding sites closer to the entrance of the outward-facing channel, which steer the ligand towards the main binding site. These initial binding sites, located at least 9 Å from the channel entrance, form fewer and weaker hydrogen bonds between glucose and the protein and therefore provide significantly less binding strength. Consequently, they do not bind glucose for longer than a few nanoseconds, unlike the central binding site where glucose resides for microseconds or longer.[58]

2.2. Targeted NP uptake mechanism

NPs are too large to pass through membrane transporters (see Fig. 1), so their cellular uptake *via* targeting mechanisms requires exofacial binding to the cell-surface receptor, followed by endocytosis.[7] Endocytosis is a well-established pathway for NP internalisation,[10,64–68] with the principal mechanisms summarised in Fig. 2a. It is also known that endocytic recycling helps cells regulate GLUTs' presence on the plasma membrane,[69,70] meaning that any NP bound to a GLUT transporter at the time of endocytosis may be co-internalised.

It should be noted that this uptake results in NPs or clusters of NPs being enclosed within intracellular vesicles (Fig. 2b).

Whilst this may suffice for diagnostic purposes or certain therapeutic approaches, it poses a limitation when the active agent must reach the cytosol or specific intracellular organelles. In such cases, the NP design must incorporate strategies for endosomal escape of the NP or its drug payload. Conversely, some therapeutic approaches, such as photothermal therapy, do not require internalisation and uptake into the cell is not even required. Instead, robust binding to the plasma membrane or membrane receptors is sufficient.[10] Thus, even targeting approaches that do not achieve NP internalisation might be of interest, though they are likely to have more limited clinical applications. In the following, we will not distinguish between NP surface binding and internalisation and refer to both effects as "uptake", since many quantification methods do not allow to make this distinction, see below.

As discussed in more detail below, it is essential to distinguish between specific targeting of glucose conjugates to the GLUT receptors, which are overexpressed in cancer and BCEC cells, and non-specific interactions with the cell membrane. The latter refers to binding which is independent of the presence of GLUTs,[71] and does not support selective cancer cell or brain targeting.

2.3. Design of GLUT targeting ligands

Glucose is generally considered the ideal targeting ligand for GLUT1, the most widely expressed transporter among cancer-associated GLUT isoforms,[46] as it is the primary substrate for this carrier. Whilst GLUT1 can also transport other hexoses such as mannose, D-galactose or xylose, these show significantly lower affinities for GLUT1.[72] Mannose could also target mannose receptors, which are highly expressed in some normal cells, potentially reducing tumour specificity.[46] A similar limitation applies to the use of other hexoses which often are used for the targeting of lectins, carbohydrate-recognising proteins that are expressed in both normal and cancer cells.[73,74]
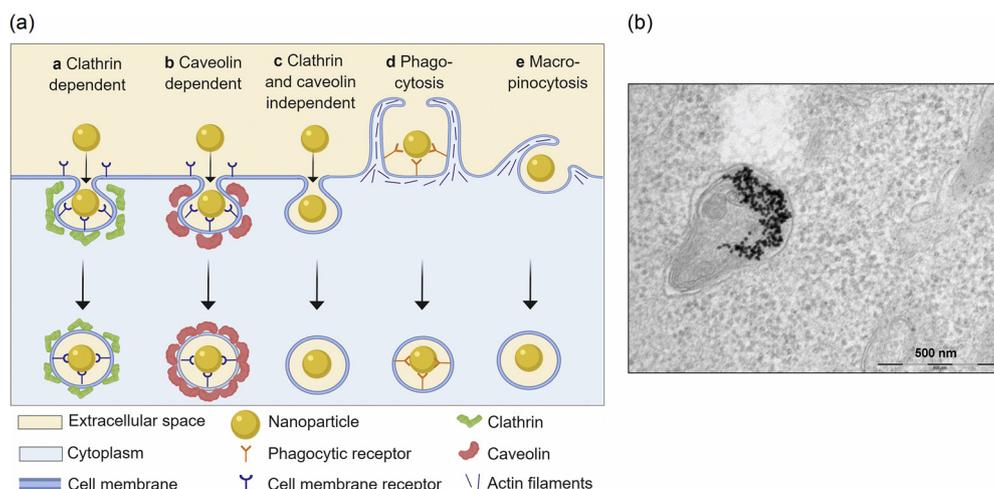

Fig. 2 Nanoparticle uptake *via* endocytosis. (a) Overview of the different endocytosis mechanisms. Reproduced from ref. 64 with permission from Elsevier, copyright 2019. (b) Transmission electron micrograph showing that gold NPs are found inside an endosome after incubation of HeLa cells with a solution of NPs. Adapted from ref. 68 with permission from the American Chemical Society, copyright 2010.

This journal is © The Royal Society of Chemistry 2026

J. Mater. Chem. B, 2026, **14**, 4874–4902 | **4877**

The design of a glycoconjugated NP capable of binding to a GLUT receptor involves several key considerations: (i) the position on the glucose ring used to form a covalent link to the NP, (ii) the length of the linker and (iii) the chemical nature of the linker. Some of these aspects can make use of the extensive work on small drug glycoconjugates that have been designed for cancer cell targeted therapy.[39,45–47] However, the size of the NPs, which prevents intrusion of the NP into the channel leading to the glucose binding site, introduces additional constraints.

The three-dimensional structure of GLUT3 in the outward-open form shows that the glucose ligand in the central binding site can form up to nine hydrogen bonds with polar amino acid residues, involving all hydroxyl and the ring oxygen,[52] although their relative importance cannot be estimated reliably from these data. There is further stabilization of the glucose by hydrophobic interactions of the glucose carbon backbone with hydrophobic residues; the importance of hydrophobic and π–π interactions for ligand binding in the main binding site has also been highlighted for GLUT1.[53] Covalently linking a functional group to one of the glucose carbons can disrupt its binding to GLUT in two ways: it may introduce steric clashes that require unfavourable structural rearrangements of the protein, and it may impair hydrogen bonding due to the removal of a hydroxyl group.

It is noteworthy that the outward-occluded GLUT3 X-ray structure contains a monoolein molecule in the narrow channel leading from the extracellular space to the binding site which forms hydrogen bonds with the C2 and C3 hydroxyl groups of glucose (see Fig. 3 for glucose carbon numbering). Although it is not expected that such a molecule is present under physiological conditions, the presence of such a long linear molecule in the crystal structure close to the glucose ligand suggests that a covalent link from one of these carbons could be easily accommodated without significant structural distortions.

Several studies have explored the effect of the removal or substitution of individual glucose hydroxyl groups on glucose binding to GLUT1. Early work indicated that the hydroxyls at C1, C3 and C4 are directly involved in glucose recognition by GLUT1, most likely by hydrogen bonding, whereas removal of the hydroxyls at C2 and C6 did not significantly affect binding, suggesting only weak interactions between these hydroxyls and the protein.[75] More recent results showed that the C1 hydroxyl

may be replaced without significantly affecting binding to GLUT1, provided a hydrogen bond acceptor is bound to C1; one notable example is glufosfamide, the only glycoconjugate which has been tested in human clinical trials.[39,47] A similar tolerance appears to exist at C4, as evidenced by 4-O-propyl-D-glucose, which retains a binding constant comparable to native glucose, whereas similar substitutions at C3 consistently reduce GLUT affinity.[47,75] Notably, C2 conjugation does not require a hydrogen bond acceptor bound to the carbon, which allows for conjugation via a wide range of conjugation strategies, including the use of the widely available 2-amino-2-deoxy glucose (glucosamine), bound to the drug molecule via a peptide bond.[76] C6 conjugation, on the other hand, appears to be less flexible. 6-Deoxy-glucose was reported to have the same GLUT1 binding constant as glucose,[75] suggesting the absence of strong hydrogen bonding between the C6 hydroxyl group and the protein. However, binding glucose C6 to the anti-tumour compound chlorambucil via a peptide bond resulted in a loss of GLUT1 recognition, whereas the same compound bound via an ester linkage showed strong GLUT1 binding,[77] suggesting the need for a hydrogen bond accepting group at C6 when conjugating at this site. The same conclusion can be drawn from a recent study comparing GLUT1 targeting by AuNPs which were conjugated to glucose at different positions.[78] A similar comparison of all positional isomers of a glucose-platinum conjugate further confirmed that C2-conjugated glucose has the highest GLUT1-mediated cell uptake, even when retaining the hydroxyl oxygen and thus the hydrogen bond accepting capability at the linker position.[79]

Overall, conjugation at C2 emerges as the most promising strategy, supported by both steric and hydrogen bonding considerations. It also seems to allow for a wider range of chemical strategies for attaching a ligand compared to other positions. These results are summarised schematically in Fig. 3.

A further feature that needs considering when designing glycoconjugated NPs is the tether between the glucose moiety and the NP, particularly its length. As discussed earlier and illustrated in Fig. 1, the GLUTs' glucose binding site is located in the centre of the protein, approximately 20 Å from the entrance of a narrow channel on the exofacial side of the protein measuring 3–4 Å in diameter.[52,59] In contrast to smaller molecules, NPs are too large to allow significant penetration into this channel. Although MD simulations suggest the existence of glucose binding sites closer to the channel entrance which help to guide the ligand towards the main binding site,[58,61–63] binding to these location is by design only transient, i.e. much weaker and short-lasting.[58] Thus, only the central binding site is expected to hold a glucose ligand for long enough to allow for endocytosis of the attached NP to take place. Therefore, the glucose moiety must be located at the end of a tether with a length of at least 20 Å to be able to reach the central binding site.

However, another issue which needs to be considered in this context is the ligand density on the NP surface. It seems obvious that increasing the number of glucose-bearing ligands on a NP should lead to increased binding to a GLUT protein or even to multivalent targeting, i.e. increased binding due to
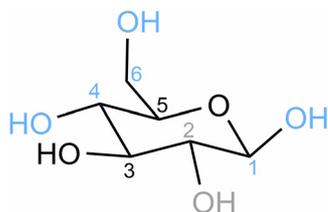

Fig. 3 Schematic structure of glucose (in the dominant β-D-glucopyranose form), showing the standard numbering of the carbons. The colours indicate where conjugation is possible without significant loss of binding to GLUT1, as discussed in the text – black: conjugation does not seem possible; light grey: conjugation possible with a wide range of different bonding strategies; light blue: conjugation possible provided that a hydrogen bond acceptor is bound to the carbon.

4878 | J. Mater. Chem. B, 2026, **14**, 4874–4902

This journal is © The Royal Society of Chemistry 2026

interactions with several GLUT targets.[80] On the other hand, if the tethered ligands form a dense monolayer on the NP surface, steric hindrance may impede their access to the narrow channel leading to the glucose binding site. This is particularly true for solid NPs, NPs with low surface curvature (*i.e.* larger NPs) and for the case of ligands that are just long enough to fulfil the length criterion outlined in the previous paragraph. In contrast to solid inorganic NPs, polymeric or micellar NPs provide some additional flexibility of the NP core to reduce such steric hindrance. However, in general in may be advisable or even necessary to use a tether that is longer than the minimum length discussed above or to inter-sperse glucose-bearing ligands with shorter ligands that act as spacers to enhance the chances of successful targeting.

It is also interesting to speculate on the nature of the ideal tether. The exofacial channel leading to the binding site is lined by many polar residues with hydrogen bonding capability, which form transient glucose binding sites and hence support glucose transport to the main binding site.[58] This suggests that a hydro-philic linker could further strengthen NP binding by forming additional hydrogen bonds to the residues in the channel. On the other hand, as discussed above, hydrophobic interactions have been shown to make significant contributions to the glucose binding affinity of GLUTs and thus may also contribute to increased binding due to tether interactions. The GLUT3 X-ray structure contains the hydrocarbon chain of a monoolein mole-cule in the exofacial channel, which shows that hydrophobic moieties can be well accommodated in this channel. It has been shown that conjugation of different moieties to glucose and other hexoses can lead to a significant enhancement of binding to GLUTs, reducing the dissociation constant from the mM to the μM range. Such effects have been reported for small glycoconju-gates of different drug molecules[77,81] as well as aromatic fluores-cence markers.[82–85] For example, conjugation of hydrophobic chlorambucil to glucose was found to increase the binding to GLUT1 by a factor of 150.[77] This highlights that both hydrophilic and hydrophobic interactions of the tether may further strengthen binding of glucose conjugated NPs to GLUTs. The tether may also affect the targeting specificity of glycoconjugates; for example, it has been suggested that a more hydrophilic tether reduces unspecific uptake through the hydrophobic cell membrane, which is the dominant mechanism for uptake of smaller glycoconjugates into cells with low GLUT expression, thus improving the specific targeting of GLUT-rich cells.[86] Although the uptake of larger NPs is not expected to proceed through the cell membrane, unspecific binding and subsequent uptake by endocytosis may be affected in a similar manner. As to tether topology, a flexible linear tether, such as a polyethylene glycol (PEG) chain, is likely ideal to minimise steric hindrances, although the channel's diameter is sufficient to accommodate short side chains or small aromatic rings.

3. Confirmation of GLUT targeting

Numerous studies have investigated the cellular uptake of glycoconjugated NPs into cancer cells or other cells which overexpress GLUTs, using a wide range of methods to confirm or even quantify cellular uptake.[65] One elegant approach involves the use of fluorescent NPs, either intrinsically emissive or labelled with a fluorescent dye. This enables visualisation by fluorescence microscopy, which can also reveal the intracellular localisation of the internalised NPs; Fig. 4a shows the principle of fluorescence microscopy and Fig. 4b presents images of Rhodamine-B-labelled glucose-functionalised AuNPs taken up into different cells as an example for the use of this method. However, this method is limited to the analysis of a relatively small number of cells. For larger-scale quantification of the cellular uptake of fluorescently labelled NPs, flow cytometry is commonly used. The principle of the method is illustrated in Fig. 5a, with representative data demonstrating NP–cell inter-actions shown in Fig. 5b. Another widely used method deter-mines the average amount of a specific element (*e.g.* gold for AuNPs) associated with each cell using methods based on the vaporization of cells in an inductively coupled plasma (ICP) and detection of elements based on their optical emission spectra (ICP-OES, Fig. 6) or mass (ICP-MS), or using flame atomic absorption spectroscopy (FAAS). Direct visualisation of the NPs may also be achieved by transmission electron microscopy (TEM), although quantitative estimates of NP uptake from TEM images are limited.[65] Techniques such as fluorescence microscopy or TEM can differentiate between internalisation of the NPs into the cell and association with the plasma membrane without internalisa-tion. However, in other assays, this distinction requires additional pre-treatment steps, such as enzymatic or chemical removal of surface-bound, non-endocytosed NPs.[87] In a few cases, a more specific method has been used, such as measuring drug release inside cells from a drug-loaded nanocarrier.

However, many of the publications that report cellular uptake of glycoconjugated NPs did not investigate the question whether this uptake was mediated by the GLUT target, which is a requirement for targeted cancer treatment. NP endocytosis can also occur upon unspecific interactions with the plasma membrane (adsorptive-mediated endocytosis) or other membrane components which are not characteristic of cancer cells. The same concern applies to glycoconjugated small-molecule drugs, even though the uptake mechanisms may differ. Prior reviews of such glycoconjugated drugs have highlighted that this question often remains unresolved in the literature, even for well-studied molecules.[39,45,46,93] Notably, it has been proposed that com-monly used fluorescent glucose analogues, such as 2-NBDG and 6-NBDG, which have been used for GLUT assays, might occur by mechanisms that do not make use of GLUTs.[71] In the following, we discuss in some more detail the different approaches that have been used in an attempt to show that glycoconjugated NP uptake is due to their interaction with GLUTs.

3.1. Comparison of NPs with different ligands

Many studies in the field compare NP uptake before and after glycoconjugation or before and after replacing the original capping layer with one containing a glucose derivative. It must be stressed that the results of such experiments alone are of highly limited value for deciding if a particular glycoconjugation
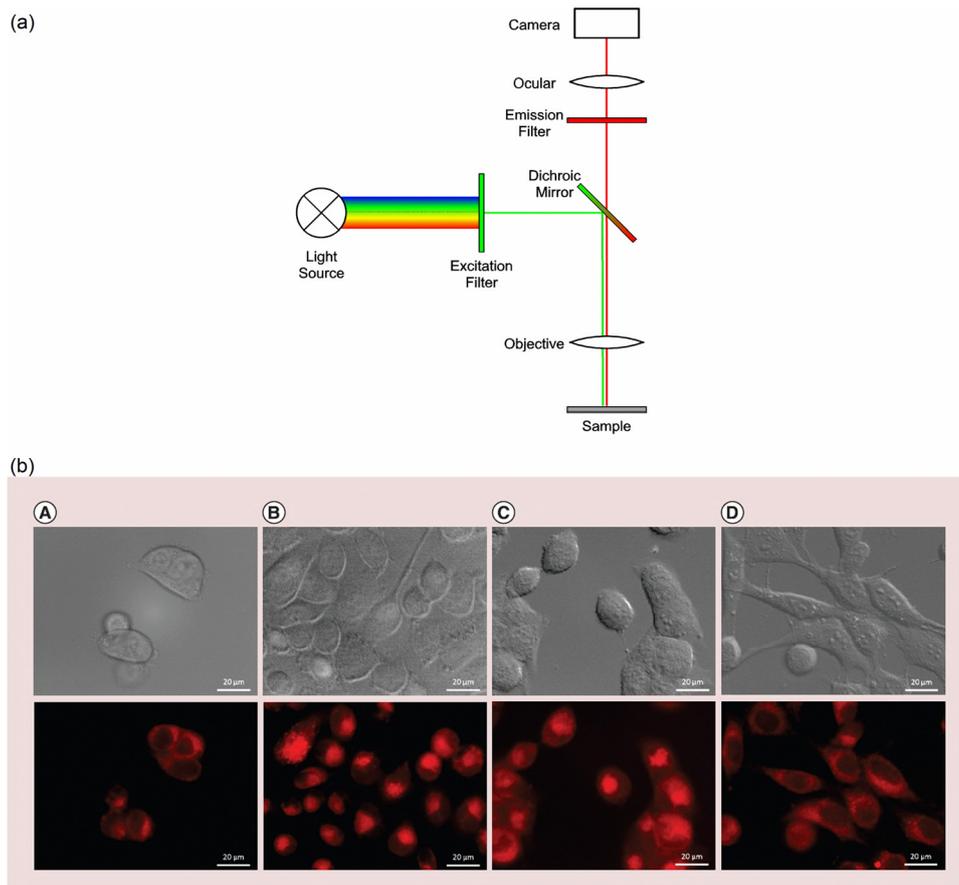
This journal is © The Royal Society of Chemistry 2026

J. Mater. Chem. B, 2026, **14**, 4874–4902 | **4879**

Fig. 4 Fluorescence microscopy. (a) Principle of a fluorescence microscope, showing the excitation and fluorescence light paths in green and red, respectively. If a laser is used as excitation light source, there is no need for an excitation filter. (b) Cellular uptake of AuNPs, detected by fluorescence. (A) A431 cells; (B) A549 cells; (C) LNCaP cells; and (D) 3T3 cells, treated with Rhodamine B-conjugated and glucose-functionalised AuNPs. Top: Bright field image. Bottom: Rhodamine B fluorescence (red). Scale bar: 20 μm. Fig. 4b reproduced from ref. 88 with permission from Informa UK Limited, trading Taylor & Francis Group, copyright 2018.

method does have the potential of directing the NPs to GLUT-rich cells, since changes to the NP capping layer alone can significantly affect NP uptake by cells, even in the absence of any specific interaction with GLUT proteins. In particular, glycoconjugation may alter the surface charge of NPs,[8] which is known to affect unspecific binding and hence uptake of NPs by adsorptive-mediated endocytosis, with negatively charged NPs generally having lower uptake due to their repulsion by the negatively charged plasma membrane.[87,94] Additionally, introducing polymer or peptide coatings can significantly affect the ability of NPs to form a protein corona which influences their tendency for adhering to the cell surface or internalisation through endocytosis.[10,65–67,95] Thus, an observed increase in NP uptake following glycoconjugation alone is not sufficient evidence for GLUT-mediated targeting or cancer cell recognition.

A more meaningful approach involves comparing glycoconjugated NPs that differ only in the conjugation positions on the glucose ring. As discussed, the ability of glucose derivatives to bind to GLUTs is affected strongly by the location of the covalent link to the glucose ring (Fig. 3). Modifications at the C3 hydroxyl lead to significantly impaired binding, whereas covalently linking C2 or C6 appears to affect glucose binding to

GLUTs to a much lesser extent. Thus, comparing glycoconjugated NPs that are identical in their ligand structure except for the glucose linkage position can provide direct evidence for the mediation of NP uptake by GLUTs.

3.2. Comparison of different cell lines

A widely used method for assessing the GLUT targeting potential of glycoconjugated NPs involves comparing their uptake in non-cancerous and cancerous cells (or other cells with high GLUT expression). This method relies on the assumption that observed differences are due mostly to the different levels of GLUT expression. Although such results are obviously relevant for practical applications of the NPs investigated, it is well known that different cell lines differ in their non-specific nanoparticle binding and uptake behaviours.[65,66,88] Therefore, this approach provides at best a first indication of successful GLUT targeting and needs to be combined with one of the other methods to assess the general applicability of the glucose conjugation method used.

3.3. Glucose competition

A standard test for the propensity of glucose derivatives for binding to GLUTs are competition experiments with glucose or

4880 | *J. Mater. Chem. B*, 2026, **14**, 4874–4902

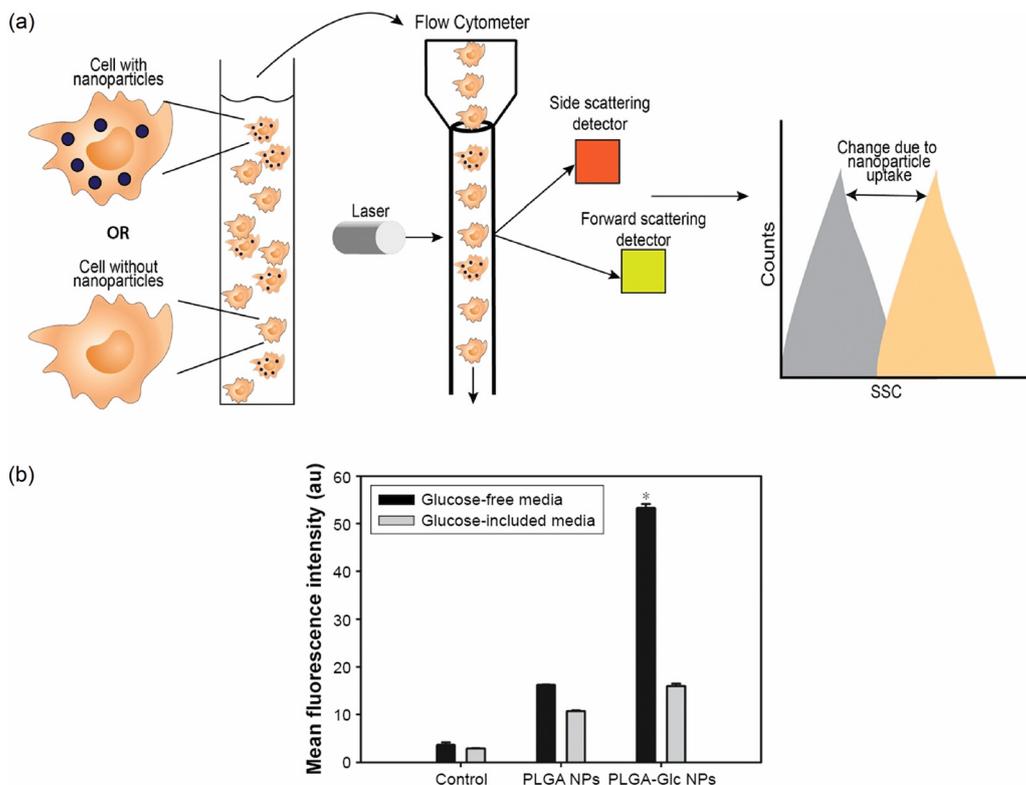This journal is © The Royal Society of Chemistry 2026

Fig. 5 Flow cytometry for the quantification of the cellular uptake of fluorescent NPs. (a) Schematic depicting flow cytometry. A diluted cell suspension flows through a microfluidic tube, allowing the detection of fluorescence from individual cells by the side scattering detector. The distribution of fluorescence intensities (SSC) from individual cells reflects the uptake of fluorescing NPs, as depicted schematically. Reproduced from ref. 89 with permission from Elsevier, copyright 2023. (b) Cellular uptake of fluorescently labelled poly((D,L)lactic–glycolic) acid (PLGA) NPs without or with glucose functionalization (-Glc) upon incubation of Hep-2 cells in the absence or presence of excess glucose, observed by flow cytometry. Reproduced from ref. 90 with permission from Dove Medical Press Ltd, Taylor & Francis Group, copyright 2017.

other sugars which are isotopically or fluorescently labelled to allow measuring their uptake.[75] This method can be adopted for glucose-conjugated NPs, without requiring labelled glucose; in the presence of high concentrations of glucose, GLUT-mediated NP binding should be competitively inhibited, resulting in reduced NP uptake. Under the assumption that the presence of glucose does not interfere with non-specific NP binding to the cell surface, which can be tested by experiments using non-glycoconjugated NPs with a similar surface chemistry, this provides strong evidence for GLUT-specific targeting. Due to the fast binding and transport of glucose via GLUTs,[96,97] there is no need for long preincubation periods with excess glucose, but the excess glucose needs to remain during NP incubation. This suggests that coincubation of the NPs and excess glucose without any preincubation is a good approach, which indeed has been shown to work,[71,83,90,98] although more often excess glucose has been added typically 30–60 minutes prior to the addition of NPs. In fact, prolonged excess glucose treatment ($\geq$24 hours) is well known to up- or downregulate a wide range of cellular functions,[99–106] which may indirectly change NP uptake, and therefore should be avoided. However, failure to observe reduced NP uptake in the presence of glucose does not definitively rule out GLUT-mediated binding. This outcome could reflect a significantly higher binding affinity of

the glucose-NP construct, potentially due to additional stabilising interactions between the glucose-linking tether and the interior of the GLUT channel. Such significantly increased GLUT binding affinities upon conjugation of sugars have been found in multiple previous studies,[77,81–85] as discussed above. In such cases, it will be necessary to undertake more extensive experiments, such as measuring NP uptake for a range of glucose and NP concentrations and to employ glucose analogues with higher GLUT binding affinities to unequivocally establish competitive GLUT binding of the glycosylated NP. Such studies should be informed by protocols that were used in studying small glycoconjugates with high GLUT affinities,[77,81–84] which included the establishment of a full screening assay for GLUT5 inhibitors.[107]

3.4. GLUT inhibition

GLUT-mediated NP uptake can also be investigated in the presence of GLUT inhibitors, which include natural compounds, such as phloretin or cytochalasin B (Cyt-B), or small chemicals, such as fasentin or WZB117.[39] If their presence, at a concentration known to inhibit the activity of the relevant GLUT, significantly reduces the measured uptake of the glucose conjugated NPs under investigation, this again provides a convincing argument for the mediation of NP uptake by the GLUT. Ideally, this should be accompanied by a control showing
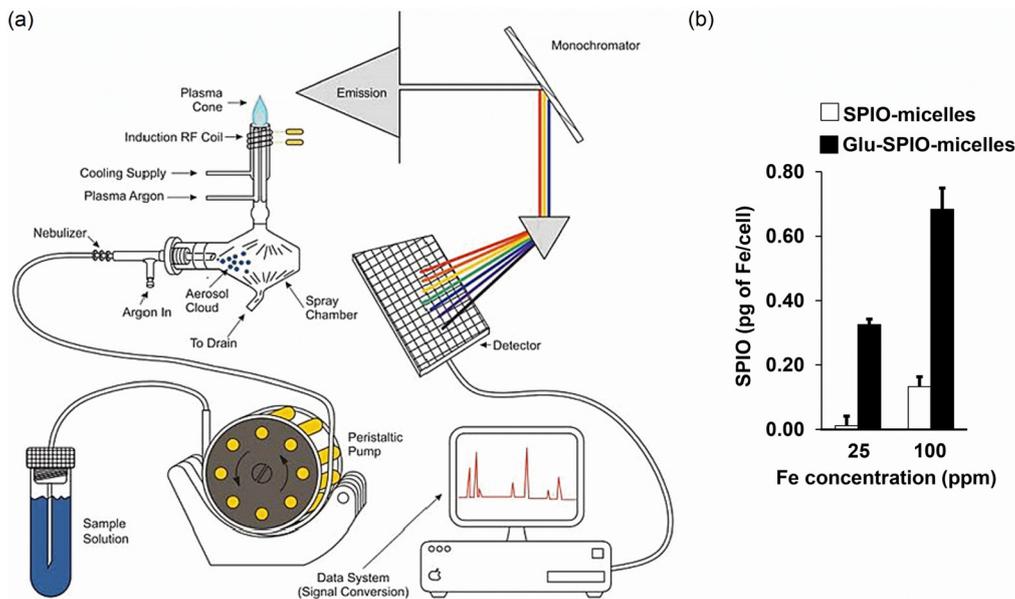
Fig. 6 ICP-OES for the quantification of cellular NP uptake. (a) Schematic representation of ICP-OES components, including plasma generation (left) and emission detection (right). Reproduced from ref. 91 with permission from Elsevier, copyright 2023. (b) Cellular uptake of superparamagnetic iron oxide (SPIO)-loaded micelles (formed from poly(ethylene glycol)-*block*-poly(ε-caprolactone)) without and with glucosamine functionalisation (Glu-) upon incubation of PC-3 cells at different micelle concentrations (expressed as Fe concentration), detected by ICP-OES. Reproduced from ref. 92 with permission from Springer Nature, copyright 2017.

no significant effect on the uptake of non-glycoconjugated NPs to rule out indirect effects of the inhibitor on non-specific NP interactions with the membrane. The effect of GLUT inhibitors is typically observed after short incubation periods;[40,44,108–113] typically, they are added 30 minutes prior to the addition of NPs. The inhibitor should remain present during the NP incubation, since the inhibiting effect normally decreases rapidly.[78] Longer inhibitor exposure should be avoided, since they are known to interfere with many other cellular functions when applied on longer time scales,[108,114–116] and thus may have indirect effects on the uptake of NPs. As with glucose competition experiments, failure to observe an inhibitor effect does not necessarily exclude GLUT involvement. NP uptake in the presence of an inhibitor could arise from a very high binding constant of the glucose-conjugated NP, so that its binding is preferred to inhibitor binding, or from the fact that the inhibitor does not work by blocking the GLUT glucose binding site, but prevents glucose uptake by a different mechanism, such as inhibiting the structural transition from the GLUT outward-open to the inward-open conformation.

A related strategy involves anti-GLUT antibodies to block binding to GLUTs, preventing NP uptake *via* the glucose-targeted route. However, this method requires caution, since the presence of a protein at high concentrations may also alter the protein corona formed on the NP surface, which in turn strongly regulates its unspecific binding to the plasma membrane and subsequent cell uptake. In particular, the presence of serum proteins in the NP corona strongly enhances NP uptake by endocytosis,[117] so that even a partial replacement of those serum proteins in the NP corona by antibodies may affect cellular uptake. Therefore, control experiments with non-glycoconjugated NPs with a similar surface chemistry are needed to rule out such indirect effects of antibodies.

GLUT knockdown or knockout studies may further validate GLUT-mediated uptake. This is normally achieved through small interfering RNA (siRNA) mediated gene silencing or CRISPR-based gene editing, which reduces or eliminates the production of GLUT transporters at the plasma membrane.[118–120] While this can provide direct mechanistic insight, interpretation of such results must be undertaken with caution. GLUT knockdown or knockout and glucose deprivation, which is the immediate effect of reduced GLUT expression, can lead to broad effects on cell cycle and metabolism, oxidative stress pathways, and endocytic function.[104–106,121] As a result, observed reductions in NP uptake may stem from secondary cellular responses, rather than loss of NP–GLUT interaction itself. Therefore, while GLUT knockdown is a valuable tool, results must be interpreted in the context of such potential off-target metabolic effects.

3.5. *In vivo* experiments

In some reports of successful cancer cell targeting using glucose-conjugated NPs, *in vitro* experiments of the type described so far were complemented by *in vivo* experiments, showing NP accumulation in tumour tissue or targeted organs, or providing insights on the NPs' biodistribution. Other studies only report such *in vivo* results without accompanying *in vitro* experiments. Such experiments are, of course, needed for ultimately assessing the efficiency of any targeted NP design for practical applications. However, on their own they may not provide reliable evidence for successful targeting of cancer cells or GLUT receptors, since the biological response can arise from a complicated interplay of effects[122] which may hide successful targeting of the NPs to the target or produce misleading results which wrongly suggest such

4882 | *J. Mater. Chem. B*, 2026, **14**, 4874–4902

This journal is © The Royal Society of Chemistry 2026

targeting; therefore, the following review is limited to *in vitro* cellular uptake results.

4. Literature review

The aim of this literature review is to evaluate whether glucose-conjugated NPs can selectively target GLUT overexpressing cells *via* GLUT-mediated uptake. Specifically, we assess whether the observed cellular uptake of such NPs in published studies can be reliably attributed to interactions with GLUTs rather than non-specific mechanisms. To do so, we focused on reviewing the structural configuration of the glucose moiety on the NP, including the site of conjugation on the glucose ring, and the nature and length of the linker, together with any direct evidence for GLUT involvement, such as competition experiments, inhibition studies, or other valid controls previously discussed in Section 3.

To ensure consistency and relevance, we applied strict inclusion criteria. Only studies in which glucose or glucose derivatives were covalently attached to the NP surface were included, since non-covalently bound ligands are unlikely to support specific receptor-mediated uptake. We also excluded studies using unrelated mono- or polysaccharides as ligands, since they exhibit weaker binding to GLUT1, the most widely overexpressed GLUT in cancer or BCEC cells and often target other plasma membrane components. As mentioned previously, we focused exclusively on *in vitro* studies as proof of GLUT-mediated uptake; excluding studies solely reporting *in vivo* experiments (see Section 3.5).

The following sections are organised according to the nature of the glucose-NP conjugation, namely, direct attachment, short linkers, and long linkers. A summarising table of all reports reviewed here is included in the SI, which provides a few more details, such as conjugation position on the glucose ring and uptake quantification method used.

4.1. Direct glucose attachment to the NP surface

Direct attachment of glucose to NP surfaces has been explored as a strategy for facilitating cellular uptake in several studies. Given the structural constraints of the GLUT glucose binding site, the feasibility of glucose attached directly on the NP surface interacting with these transporters by binding to the binding site is highly doubtful, as discussed above. This section critically examines studies employing direct glucose conjugation.

4.1.1. Studies without GLUT targeting control experiments.
1-Thioglucose (1-TG) and its fluorinated derivative, fluoro-6-deoxy-thio-1-glucose (F-1-TG), have been directly conjugated to AuNPs through the C1 position, making use of the strong gold–sulfur affinity. The uptake of 1-TG and F-1-TG-capped Au-NPs with diameters in the range of 8–14 nm in various cancer cell lines was 1.5–4 times higher than that of citrate-capped AuNPs of the same size;[11,123–125] Fig. 7 depicts this conjugation and shows a typical result. Comparison of small Au-nanoclusters (2.6 nm diameter) with a glutathione or mixed glutathione/1-TG capping layer using fluorescence microscopy suggested higher uptake of the latter by cancer cells, but not by non-cancerous cells,
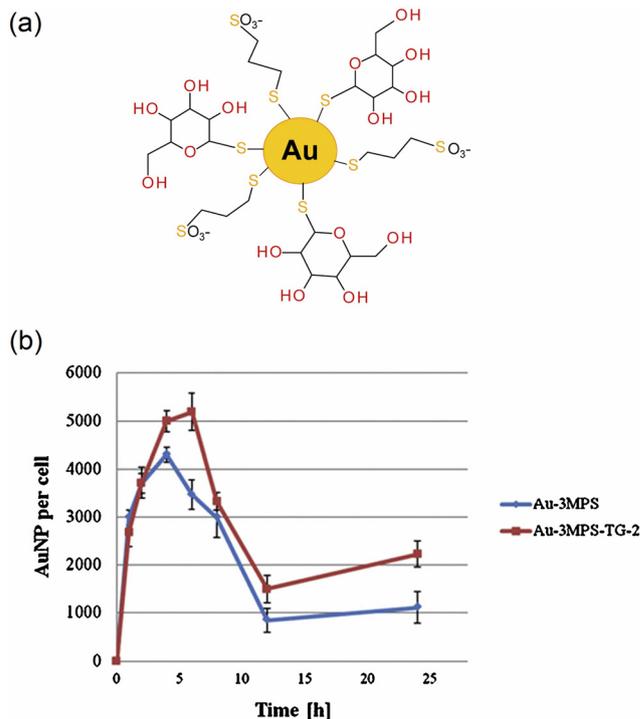

Fig. 7 Example of direct glucose attachment to the NP surface. (a) Schematic chemical structure of a AuNP coated with a mixture of 3-mercapto-1-propansulfate (3-MPS) and 1-thio-glucose (TG) (not to scale). (b) Uptake of 3-MPS-stabilised AuNPs (Au-3MPS) and AuNPs stabilised with 3-MPS and TG in a molar ratio of 6/1 (Au-3MPS-TG-2) upon incubation of HSG cells for different time intervals, detected by FAAS. Adapted from ref. 127 with permission from Elsevier, copyright 2016.

although the distinction between the different levels of NP uptake is not very clear in the images presented and no quantification was provided.[126] Similarly, 15 nm AuNPs capped with a mixed 1-TG/3-mercapto-1-propanesulfonate (3-MPS) layer showed a small (25%) increase in uptake into HSG cells (a HeLa cell-derived line) compared to AuNPs capped with only 3-MPS.[127] However, in all of these cases, the observed increase in uptake may primarily result from changes to the capping layer. Specifically, reducing the negative surface charge upon replacing all or some of the negatively charged citrate, glutathione or 3-MPS ligands by neutral 1-TG/F-1-TG in turn reduces the electrostatic repulsion between the NPs and the negatively charged plasma membrane. This is consistent with previous studies on the effect of the AuNP surface charge on cell uptake[87] and is further supported by the significantly enhanced uptake of positively charged cysteamine-capped Au-NPs found in one of those studies.[11] Similarly, 20 nm AuNPs with a mixed PEG/1-TG capping layer demonstrated an increased uptake in THP-1 leukaemia and MCF-7 breast cancer cells and improved radiosensitivity, compared to AuNPs with a PEG coating.[128] This is most likely due to the well-known fact that a PEG ligand shell prevents unspecific uptake of NPs,[117] so that a reduction of the shell's PEG content leads to increased cellular uptake.

In a similar approach, 61 nm silver NPs (AgNPs) were conjugated to glucosamine at the C2 amine group by ligand

This journal is © The Royal Society of Chemistry 2026

J. Mater. Chem. B, 2026, **14**, 4874–4902 | **4883**

exchange, whereby citrate and tannic acid ligands are replaced by glucosamine due to the strong affinity of amines for binding to silver.[129] TEM images showed uptake of glycoconjugated and non-glycoconjugated AgNPs into Du-145 and PC-3 prostate cancer cells to a similar extent and various *in vitro* tests, including NP toxicity, also showed similar results for both types of NPs, suggesting that there is no specific interaction of the glycoconjugated NPs with GLUTs.

A minor increase (30–50%) of uptake of silica coated CoFe magnetic NPs (∼200 nm diameter) into breast cancer cells (MDA-MB-231 and MCF-7) and normal breast cells (MCF-10A) was observed upon conjugation of their carboxylated surface with glucosamine at the C2 position.[130] However, again the glycoconjugation caused a significant reduction of the negative surface charge, which on its own would be expected to result in an increased cell uptake.

Direct conjugation of glucose to CdTe/CdS core–shell QDs with a diameter of 3–7 nm resulted in a significant, albeit not quantified, increase in NP uptake into living yeast cells.[131] However, this could easily be due to different unspecific binding of NPs with different surface chemistries to the cell membrane rather than specific interactions with GLUT receptors.

No increase of uptake into HeLa or cancer cells was reported for mesoporous silica nanoparticles (250–300 nm diameter) after direct conjugation of glucose at its C6 position, as opposed to the increased uptake found when glucose was bound to the end of a poly(ethylene imine) (PEI) capping layer on similar NPs (see below).[132]

No control experiments were undertaken in any of the studies described so far to investigate the involvement of GLUT receptors, *e.g.* using glucose competition experiments, linking at different glucose carbons, or using GLUT inhibitors or GLUT knockout cells. Instead, they relied on the comparison of glycoconjugated and non-glycoconjugated NPs, which does not provide reliable evidence for GLUT targeting since the modified surface properties alone can significantly affect unspecific cell uptake. A few of the studies compared uptake into cancer and non-cancer cells, but this also does not provide evidence of GLUT involvement, as discussed above.

4.1.2. Studies with GLUT targeting control experiments. There have been a few publications on NPs with glucose directly attached to the surface where the involvement of GLUTs was addressed directly by one of the methods mentioned above.

Multiwalled carbon nanotubes (MWCNTs, 180 nm hydrodynamic diameter) glycoconjugated by direct attachment of glucosamine, at its C2 amine group, were shown to be taken up into MDA-MB-231 breast cancer cells.[133] However, no comparison was made with non-glycosylated MWCNTs or cells with lower GLUT expression, making GLUT involvement uncertain. The only indication of GLUT participation was a slight decrease in uptake in the presence of excess free glucosamine, but this was contradicted by the lack of effect from the GLUT1 inhibitor Cyt-B. Given the significant aggregation of MWCNTs under the incubation conditions, changes in media composition may have influenced uptake *via* non-specific interactions.

A more recent report suggested that 1-TG capped small Au-nanoclusters (2.5 nm diameter) had significantly higher uptake into MDA-MB-231 cancer cells than similar Au-nanoclusters capped by glutathione, and the involvement of GLUT1 was suggested by a decrease of this uptake in the presence of GLUT1 inhibitor Cyt-B.[109] However, this conclusion was partly contradicted by a five-fold increase in uptake of the 1-TG capped NPs upon addition of glucose at a concentration of 18 mM, which is comparable to the glucose-GLUT dissociation constant,[134] and therefore should have resulted in significant competition between glucose and NP binding, thus reducing NP uptake. On the other hand, in light of the size distribution of these NPs, which included a measurable fraction of NPs with a diameter of less than 1.5 nm, it is possible that the smallest NPs in this preparation might be able to enter the top of the narrow channel leading to the glucose binding site of the GLUT receptor and thus are able to bind even in the absence of a long tether.

4.1.3. Conclusion. Overall, there is no conclusive evidence showing that direct attachment of glucose to a solid NP surface can provide targeting of NPs with a diameter larger than 1–2 nm to cancer or BCEC cells. This is in line with the expectation discussed above that glucose needs to be bound to the NP of that size *via* a tether with a length of at least 20 Å to reach the GLUT binding site effectively.

4.2. Glucose attachment *via* short linker

The studies discussed in this section did attempt to conjugate glucose to the NPs by covalent bonding *via* a short linker molecule. The linker length stated here represents the number of bonds between the glucose ring and the nanoparticle surface; in this section, only studies with a linker length of at most 15 bonds are included, attempts using longer linkers are summarised in Section 4.3.

4.2.1. Studies without GLUT targeting control experiments. Again, many of the studies using a short linker for conjugating glucose to a NP did not include conclusive evidence of successful GLUT targeting.

4.2.1.1. Inorganic nanoparticles. Glucose was conjugated at the C1 position to 80 nm AgNPs *via* 4-aminothiophenol (7 bonds); this resulted in an increased uptake into A549 cancer cells, compared to citrate-capped NPs, whereas the uptake into non-cancerous L929 cells was not increased.[135] However, uptake varied strongly with incubation time, with initial uptake being faster in non-cancerous cells, suggesting the endocytic mechanism to be independent of GLUT expression. Based on results with lactose-conjugated AgNPs, the authors in fact suggest that glycoconjugation influenced protein corona formation, impacting unspecific NP interactions with the plasma membrane rather than receptor specificity. Uptake of 54 nm AgNPs into HepG2 and Neuro2A cells was found to decrease upon glucose conjugation *via* thiopropionic acid (6 bonds), compared to citrate-capped NPs, in spite of the reduced negative charge of the glycoconjugated NPs.[136]

Gold/iron oxide shell/core NPs (diameter ∼5 nm) were covered with the amphiphilic polymer poly(maleic anhydride-*alt*-1-octadecene) (PMAO) and functionalised with either PEG (MW 750) or glucose at its C1 position *via* an 8-bond linker; the

4884 | *J. Mater. Chem. B*, 2026, **14**, 4874–4902

This journal is © The Royal Society of Chemistry 2026

latter showed higher uptake into HeLa cells.[137] Similarly, iron oxide NPs (6 nm diameter) with a PMAO polymer shell were functionalised by attachment of glucose (C1 position), galactose and PEG via a short linker (~ 8 bonds) to the carboxylate groups formed on the PMAO shell upon transfer into water. The uptake of glucose-functionalised NPs by Vero cells, a monkey kidney epithelial cell line, was found to be significantly higher than that of PEG-functionalised NPs, at least for NPs with a higher degree of functionalisation.[138] However, it is well known that a PEG ligand shell prevents unspecific uptake of NPs,[117] and hence there is no indication that the uptake of these glucose-functionalised NPs was mediated by GLUT receptors.

7 nm silicon NPs (Si-NPs), capped with various carbohydrates via a short linker (6 bonds between the Si-NP and glucose at the C2 position), showed greater uptake in cancer cells (SK-MEL-28, A549, MCF-7) than non-cancerous cells (MDCK, HHL5).[139] However, glucose-bound Si-NPs exhibited lower uptake than galactose-bound Si-NPs and similar uptake to mannose-bound Si-NPs, although these two carbohydrates have approximately 10 times lower binding constants for GLUT1 or GLUT2 than glucose.[72] A lower GLUT binding constant of the ligand is expected to result in less efficient NP targeting of GLUT-overexpressing cells, as has been shown explicitly for liposomes conjugated to mannose or glucose via a long PEG-linker.[140] This suggests that for the Si-NPs described here uptake is not GLUT-mediated, aligning with the authors' suggestion that galectins may act as overexpressed receptors in certain cancer cells. Similarly, conjugation of glucose at the C1 position to 4 nm Si-NPs via a linker consisting of 10 bonds resulted in significantly higher uptake into HeLa cells compared to the original carboxylate-capped Si-NPs.[141] However, this conjugation also resulted in a change of the NPs' surface charge to a significantly less negative value, which will affect the unspecific binding of the NPs to the cell surface,[87,94] limiting any conclusion that can be drawn from this observation.

Gd^{3+} loaded mesoporous silica NPs (130 nm diameter) were conjugated to glucosamine at the C2 position using an 8-bond linker, which resulted in an increase of uptake into HT1080 cells by a factor of three.[142] However, a lack of characterization of the Gd^{3+} loaded NP properties before glycoconjugation, particularly their size and surface charge, prevents ruling out non-specific interactions as the cause of increased uptake, since these parameters are known to affect NP uptake.[87,94,143] A comparison of lanthanide NPs conjugated with different monosaccharides via a 6-bond linker showed much higher uptake into RAW264.7 and HeLa cancer cells for glucose (conjugated at C1) than mannose, galactose, fucose or N-acetylglucosamine as ligands, although no uptake was observed at all for MKN-45 cancer cells.[144] However, the glycoconjugated NPs were reported to aggregate in aqueous solution and no further characterisation, such as surface charge analysis, was undertaken. In the absence of any other control experiments, it is therefore not possible to draw reliable conclusions on GLUT targeting as compared to unspecific binding to the cell surface.

Shell–core ZnS-CdSe QDs with diameters of a few nm, with a polyacrylate coating and functionalised with maltose, i.e. a

disaccharide consisting of two glucose units, were shown to bind significantly to HeLa cells.[145] However, QD functionalisation with dextran, a glucose based polysaccharide, did not show the same effect, which led the authors to conclude that this binding is non-specific. Similarly, conjugation of glucosamine, at the C2 amine group, to mercaptosuccinic acid capped 3–5 nm CdSe QDs (5 bond linker) resulted in a two-fold uptake increase into (non-cancerous) HEK293T cells,[8] but the authors state explicitly that this is due to the change of the QD surface charge upon conjugation, as verified by a change of the zeta-potential from a negative to a slightly positive value, and not due to glycoconjugation. A similar conjugation of glutathione capped 3.6 nm Ag$_2$Se QDs with glucosamine (9 bond linker) significantly increased the uptake into MCF-7 (breast) and SW1990 (pancreatic) cancer cells, by a factor of up to 10,[146] but again the glycoconjugation resulted in a significant decrease of the negative surface charge, which seems the most likely cause of this uptake increase. Conjugation of glucosamine to 4 nm AuNPs via mercaptosuccinic acid increased the computed tomography contrast of A549 cells after incubation with NPs by a factor of three compared to citrate-capped NPs;[147] however, again it seems likely that the reduction of the negative surface charge upon replacement of (negative) citrate by (neutral) glucosamine influenced uptake rather than GLUT receptor targeting.

4.2.1.2. Organic nanoparticles. Glucosamine was also conjugated at the C2 amine group to apoferritin nanocages (12 nm) containing 4 nm AuNPs in their cavity via binding to aspartic and glutamic acid residues (4–5 bonds between the protein backbone and the glucose ring), resulting in an approximately two-fold increase of uptake into cancerous (MCF-7) and non-cancerous (MCF-10A) breast cells.[148] However, the observation that the relative uptake by cells with low and high GLUT expression remains unaltered strongly suggests unspecific uptake, with the increase again resulting from a reduction of the negative charge of apoferritin,[149] rather than from interaction with a GLUT receptor. In a similar approach, glucose was bound to the amino groups of 200 nm glutenin NPs (4–6 bonds between the protein backbone and the glucose ring) and the glycoconjugated NPs, loaded with the drug camptothecin, were shown to induce cytotoxicity in MCF-7 cancer cells.[150] However, the complete absence of any control experiments prevents any conclusions on GLUT targeting.

100 nm phospholipid/cholesterol liposomes (LIPs) were modified using n-octyl-β-D-glucopyranoside at the C1 position, resulting in a short (< 8 bonds) linker, since it is most likely that the alkyl chain is partially or even fully embedded in the LIP.[151] This modification resulted in a modest increase ($\sim 50\%$) of the uptake into HepG2 cancer cells. However, the modification also resulted in a decrease of the particle size and a slightly less negative surface charge, which may have resulted in this slight uptake increase.[87,94,143] Similarly, doxorubicin-carrying chitosan NPs (~ 200 nm diameter) had a significantly higher uptake into 4T1 cancer cells after conjugation with succinyl glucosamine at the C2 amine group, although no quantification of the effect was provided.[152] However, the doxorubicin-loaded

NPs used for the uptake study were poorly characterized, with no information on size or zeta-potential provided, which raises the question of how much these parameters change upon glycoconjugation, which in turn may seriously affect cell uptake even in the absence of direct interactions with GLUTs.[87,94,143]

Glycopolymers, *i.e.* polymers with carbohydrate side chains, have been widely investigated for their ability to bind to lectin receptors on the cell surface, which is thought to be increased by the multivalency of glycopolymers, which allows for multiple potential interactions with cell surface receptors.[93] However, since lectins are widely expressed on cancerous as well non-cancerous cells, the specificity of glycopolymers for cancer cells is expected to be lower than that of ligands presenting individual glucose groups. Despite this, glucose-bearing polymers may still interact with GLUT1, provided they meet the general requirements discussed above. This paragraph discusses two examples of polymers with short linkers between the glucose moiety and the polymer backbone, none showing any specific interaction with GLUT1, as expected, due to steric hindrance of the bulky polymer in the narrow GLUT1 channel. In one study, a series of methacrylate-based glyco-block polymers were synthesised with either glucose, galactose or fructose moieties bound to one block of the polymer backbone *via* short linkers (4–6 bonds) and used to form NPs (33–77 nm) upon conjugation with a platinum anti-cancer compound.[153] Uptake into MDA-MB-231, MCF-7 and A2780 cancer cells was found to be highest for fructose-conjugated NPs, leading the authors to speculate about the involvement of GLUT5 which has high specificity for fructose,[72] but also about the involvement of various galactose-binding receptors, whereas no suggestion for the binding mechanism of glucose-conjugated NPs was made. Notably, the fructose-conjugated NPs were significantly smaller compared to their glucose- and galactose-conjugated counterparts, which may also have affected the uptake. In another study, 11 nm iron oxide NPs were decorated with PEG (30 nm hydrodynamic diameter) and then further modified by the addition of short acrylate-based polymers bearing several glucose or mannose groups with 7–10 bonds between the carbohydrate ring C1 and the polymer backbone.[154] Modification with mannose increased the NP uptake into A450 lung cancer cells, whereas modification with glucose had no effect, which the authors took as indication of interaction with mannose receptors which are over-expressed in these cell lines.

4.2.2. Studies with GLUT targeting control experiments. The following studies further characterized GLUT-targeting by employing various GLUT inhibition strategies.

Glucose conjugation has been investigated as a strategy for overcoming the BBB, due to high GLUT1 expression in brain capillary endothelial cells (BCECs). 2 nm Au-NPs decorated with mercaptoethoxy-glucose (5 bonds) allowed significantly increased transport through BCECs compared to non-brain endothelial cells.[155] In comparison, the same AuNPs linked to glutathione showed lower transport efficiency. However, GLUT1-inhibitor Cyt-B had no effect and the authors concluded that transport efficiency differences arose from variations in surface charge or the different properties of the glycocalyx of BCECs compared to that of endothelial cells from other tissues rather than GLUT-specific binding.

Cobalt ferrite magnetic NPs (27 nm) were functionalised with glucose or a fluorescent analogue *via* esterification to the citrate capping layer (7–8 bond linker), resulting in higher uptake into MCF-7 and MDA-MB-231 cancer cells than the unmodified citrate capped NPs.[156] This uptake increase might be due to the effect of the decreased negative surface charge which is expected to result from the glycoconjugation, but the authors suggested the involvement of GLUT1, based on the results of glucose competition and GLUT1 inhibition experiments. The presence of glucose at high concentration (25 mM) reduced the uptake of the glycoconjugated NPs, but only in MCF-7 cells which have low GLUT1 expression levels and not in the MDA-MB-231 cells which express GLUT1 at a four times higher level. The authors ascribe the absence of a glucose effect on the latter cells by higher expression of GLUT1 in the presence of high glucose, counteracting the competition effect, but their own results show no significantly increased GLUT1 expression after 24 hours in high glucose conditions, when NP uptake was investigated. It seems much more likely that the difference between NP uptake in low and high glucose conditions resulted from the fact that cells had been grown in those conditions for 24 hours, which is known to up- or downregulate a wide range of cellular functions,[99–106] which may indirectly affect NP uptake, as discussed above; in particular, MCF-7 cells and MDA-MB-231 cells are known to respond differently to high glucose levels.[103] The putative GLUT1 inhibitor STF-31 significantly reduced glyco-conjugated NP uptake, but only after incubation for 6 hours (MCF-7 cells) or 16 hours (MDA-MB-231 cells). This contrasts with the normally rapid action of GLUT inhibitors, which are known to also interfere with other cellular functions when applied on longer time scales, as discussed above.[108,114–116] This suggests the possibility of an indirect effect rather than inhibition of GLUT1. In fact, it has been shown that at the low concentrations used here STF-31 does not act as a GLUT1 inhibitor and reduced glucose uptake is only observed after STF-31 induced inhibition of glycolysis and mitochondrial oxidative metabolism *via* targeting of nicotinamide phosphoribosyl transferase (NAMPT) on the time scale of 10 hours or longer;[108,115,116] STF-31 acts as (rapid) GLUT1 inhibitor only at concentrations above 50 μM, but not at 5–10 μM as used here.[108] Therefore, it seems more likely that the effect of decreased NP uptake in the presence of STF-31 on the time scale of 6–16 hours which was reported here is an indirect result of NAMPT inhibition rather than interference with GLUT1 targeting; this is further supported by a report showing that MCF-7 cells are more sensitive to the presence of STF-31 at these concentrations than MDA-MB-231 cells.[157] Decreased uptake of glycoconjugated NPs was also found 72 hours after initiating gene silencing of GLUT1 by siRNA, but it has to be noted that the significantly reduced levels of GLUT1 expression effectively lead to intracellular glucose starvation, which is known to affect a wide variety of cellular functions and cell viability, particularly in cancer cells,[104–106] so that indirect effects cannot be ruled out. Neither GLUT1 inhibition method was tested on non-glycoconjugated NPs as control.

A series of reports described significantly increased uptake of glucosamine-functionalised iron oxide NPs ($\sim$10 nm) into

4886 | *J. Mater. Chem. B*, 2026, **14**, 4874–4902

This journal is © The Royal Society of Chemistry 2026

cancer cells but not non-cancerous cells after conjugation of glucosamine at the C2 position to the dimercaptosuccinic acid capping layer (6–7 bond linker).[158–160] Although this modification reduced the negative surface charge of the NPs, which may affect cellular uptake, the addition of anti-GLUT1 antibodies significantly reduced the uptake,[158,159] Fig. 8a, and excess glucose completely reverted the uptake increase,[160] Fig. 8b, which suggests binding to GLUT1 as the main reason for the increased uptake. However, close inspection of the TEM images[158,159] suggests the presence of a measurable number of NPs with a diameter of a few nm or even less, see Fig. 8c, which may indeed be able to enter the top of the narrow channel leading to the glucose binding site of the GLUT receptor, bringing them close enough to allow glucose binding *via* a shorter tether.

Uptake of nanospheres and nanofibers formed from self-assembled peptide amphiphiles into MCF-7 cancer cells was investigated using fluorescein-labelled oligonucleotides which bind to these nanostructures by electrostatic interactions.[161] Oligonucleotide uptake was found to occur within minutes of exposing cells to nanospheres (50–100 nm diameter), and this uptake was independent of conjugation of glucose at the C1 position to the nanospheres or the presence of endocytosis or GLUT1 inhibitors. This suggests direct transport of the oligonucleotide into the cell after detachment from the nanospheres, which have a close to neutral surface charge, rather than uptake of the NPs. The nanofibers (10 nm diameter, several 100 nm length), on the other hand, have a significant positive charge and therefore are able to bind negatively charged oligonucleotides more strongly. Their uptake was found to occur on the time scale of hours and was shown to proceed *via* endocytosis. Glucose conjugation to the nanofiber surface increased their uptake by a factor of two, but the presence of GLUT1-inhibitor Cyt-B affected the uptake of non-glucose conjugated and glucose conjugated nanofibers to the same extent. On the other hand, an inhibitor of the sodium dependent glucose transporter SGLT1 affected only the latter ones, leading the authors to conclude that glycoconjugation leads to the specific interaction of the nanofibers with SGLT1, but not with GLUTs. The latter observation may be related to the insufficient length of the linker between glucose and the hydrophobic core of the
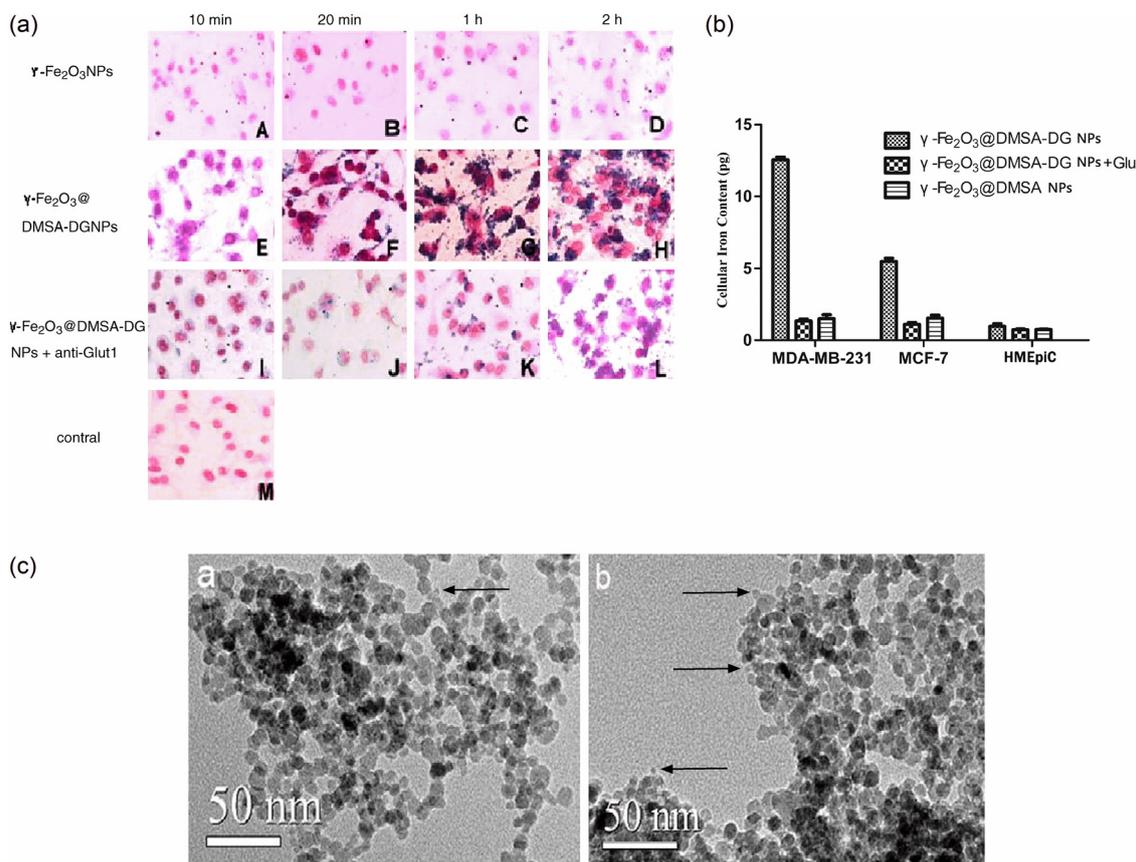
Fig. 8 Uptake of iron oxide NPs with a dimercaptosuccinic acid (DMSA) capping layer without or with conjugation of glucosamine (DG) to DMSA. (a) Microscopic images of MDA-MB-231 cells after incubation with NPs for different time intervals: NPs without glycoconjugation (A–D); NPs with glycoconjugation in the absence (E–H) and presence (I–L) of GLUT1 antibodies. NPs were stained using Prussian blue and nuclei were counterstained with red dye. Reproduced from ref. 158 with permission from Elsevier, copyright 2012. (b) Quantification of NP uptake upon incubation of different cell lines (MDA-MB-231, MCF-7 and HMEpiCs) for 30 min in the absence and presence of excess glucose (Glu), as determined by an ultraviolet colorimetric assay. Reproduced from ref. 160 with permission from Springer Nature, copyright 2016. (c) TEM images of iron oxide NPs with a DMSA capping layer without (left) and with (right) glucosamine functionalisation. The arrows indicate some examples of very small NPs. Adapted from ref. 158 with permission from Elsevier, copyright 2012.

This journal is © The Royal Society of Chemistry 2026

J. Mater. Chem. B, 2026, 14, 4874–4902 | 4887

nanofibers, preventing the binding of the glucose moiety to the GLUT binding site.

4.2.3. Conclusion. We have not been able to find any reports which conclusively demonstrated that conjugating glucose to NPs that are larger than 2 nm *via* a short linker of 15 bonds or less significantly increases their uptake into cancer or BBB cells *via* binding to GLUT1. This further confirms the conclusion of Section 2, that the linker between the glucose moiety and the NP needs to have a length of at least 20 Å, so that the glucose can reach the central binding site of the GLUT receptor when the NP is not able to significantly penetrate into the narrow channel leading from the receptor surface to the binding site.

4.3. Glucose attachment *via* long linker

This section includes a critical review of studies utilising long linkers to attach glucose or its derivatives to the NP. For solid NPs, such linkers are often introduced explicitly to allow glucose to reach the GLUT binding site *via* the narrow channel with a length of 20 Å on the exofacial side of the GLUT receptors, see Fig. 1. In contrast, polymeric NPs, owing to their often less well-defined surface, can achieve similar effective linker lengths by conjugating glucose to one of the polymer's terminals without the introduction of a specific linker, unless the synthetic protocol requires it.

4.3.1. Studies without GLUT targeting control experiments. Similarly to the work described in Sections 4.1.1 and 4.2.1, many of the studies using long linkers between the NP and glucose suggested successful GLUT targeting without providing conclusive evidence.

4.3.1.1. Inorganic nanoparticles. 13 nm AuNPs were shown to have significantly higher uptake into RAW264.7 and peritoneal macrophages after functionalisation of their zwitterionic ligand shell with glucosamine at its C2 amine (18 bonds).[162] However, the authors explicitly point out that this was likely due to a shift in surface charge from negative to positive, which promotes the NPs' interaction with the negative plasma membrane.

Fluorescent CdTe/CdS core/shell QDs with a diameter of 4 nm and capped with glucose-phenyl diamine disulfide ligands (18 bonds, glucose conjugated at C1) were shown to have an approx. 3 times higher uptake into hepatic cancer cells (HepG2) than the same NPs capped with tetraethyleneglycol.[163] The authors speculated that this might be due to GLUT binding, but it seems more likely that the ethylene glycol ligand shell reduces unspecific uptake, as it is well known that PEG ligand shells prevent unspecific uptake of NPs.[117] Therefore, in absence of any other control experiments testing for the involvement of GLUTs, these results do not provide conclusive support for successful targeting of cancer cells by interaction with GLUT receptors.

4 nm carbon dots were synthesised from glucose by hydrothermal carbonization and therefore were likely to have "surface functional groups similar to glucose" at the end of an unspecified polymeric tether.[164] Using yeast mutant strains in which all glucose transporters are expressed or deleted, it was shown that carbon nanodot uptake into yeast cells required the

presence of the yeast glucose transporters,[165] which are homologues of the mammalian GLUT transporters.[166] Although this gives some indication of the feasibility of GLUT targeting by NPs with glucose at the end of a longer linker, the evidence is indirect at best. The lack of any control beyond a comparison between yeast strains with different glucose transporter expression but described as having a "similar genetic background"[165] does preclude any definitive conclusions.

Iron oxide NPs (10–30 nm) carrying chlorine e6 as photodynamic agent were shown to have three times higher uptake into Lewis (murine cancer) cells after conjugation of glucosamine at the C2 amine group to the end of the polyglycerol chains covering the NPs.[167] Slightly less uptake of the glycoconjugated NPs was observed in non-cancerous (16HBE) cells, but this was the only control experiment presented here, which on its own is not sufficient to support any conclusion on successful GLUT targeting; in particular, no information was provided on the size or surface charge of the non-glycoconjugated control NPs carrying Ce6, both of which are known to have strong effects on NP uptake.[87,94,143]

For relatively large (200–400 nm) mesoporous silica nanoparticles a minor increase (∼50%) of uptake into HeLa and A549 cancer cells was reported after conjugation of glucose at the C6 position to the end of a poly(ethylene imine) (PEI) capping layer[132] and doubling of the uptake was found for MDA-MB-231 breast cancer cells.[168] Although the PEI capping ligand length was not specified, it seems likely that it was long enough for the glucose moiety to reach the GLUT binding site, whereas direct attachment of glucose to the silica nanoparticles did not yield a noticeable effect on NP uptake for any of these cells. This might suggest that the observed effect indeed arose from interaction with GLUT receptors; however, no control experiments, such as glucose competition or the use of GLUT inhibitors, were reported, and for most cell types the PEI capping layer itself had a much larger effect on NP uptake than the subsequent addition of glucose, most likely due to its strongly positive charge, so that any such conclusions can at best be described as tentative.

MWCNTs (110 nm hydrodynamic diameter) decorated with glucosamine (C2) *via* a long PEG-phospholipid linker, showed significant attachment to the surface of MDA-MB-231 breast cancer cells.[133] However, there was no comparison with non-glycoconjugated MWCNTs or with their interaction with cells with lower GLUT expression, the addition of the GLUT1 inhibitor Cyt-B had no effect and excess free glucosamine (10 mM) had only a minor effect, which makes is seem unlikely that this uptake was mediated by GLUTs.

4.3.1.2. Polymeric nanoparticles. Single-chain polymer nanoparticles (1.9–3.4 nm), glycoconjugated with glucose or methyl glucoside, were shown to be taken up into HeLa cells.[169] Uptake was reduced by a factor of 2 when glucose was conjugated at C1, compared to conjugation at C6, which in the absence of control experiments with non-glycoconjugated NPs or any glucose competition or GLUT inhibition experiments is the only indication of GLUT involvement, since conjugation at different positions of the glucose ring is known to affect GLUT binding

4888 | *J. Mater. Chem. B*, 2026, **14**, 4874–4902

This journal is © The Royal Society of Chemistry 2026

differently, compare Fig. 3. However, this is only a weak argument, especially since NPs with glucose bound at C1 also had a smaller size than those with glucose bound at C6, which is expected to contribute to the unspecific uptake efficiency.[143]

Conjugation of glucosamine at its C2 amine group to the termini of polyether-copolyester dendrimers (7–11 nm hydrodynamic diameter) led to an 8-fold and 2-fold increase in uptake into U87-MG and U343-MGa glioma cells, respectively.[170] This modification also enhanced the toxicity of the methotrexate (MTX) anti-cancer payload and increased transport across a BBB model. Similarly, conjugation of glucose to the ends of poly(amidoamine) (PAMAM) dendrimers (12–20 nm) increased their uptake into MDA-MB-231 cancer cells, but not into noncancerous HaCaT cells, and also increased the toxicity of their MTX payload.[171] Mesoporous silica NPs, coated with PAMAM dendrimers and loaded with the anti-cancer drug deferasirox, (88 nm) showed increased toxicity toward Y79 cancer cells following conjugation of glucuronic acid to the PAMAM dendrimers.[172] However, in the first two of these studies glycoconjugation also resulted in an increase of the hydrodynamic diameter and potentially other properties of the dendrimers. For the third study, insufficient information was provided regarding the impact of glycoconjugation on nanoparticle size. Therefore, in the absence of any control experiments, nonspecific uptake effects cannot be ruled out.

Poly(lactic-co-glycolic acid) (PLGA) NPs (100 nm) were shown to have significantly higher uptake into HT-29 colon cancer cells after functionalization with glucosamine (uptake not quantified).[173] Glycoconjugation did not significantly affect the size or surface charge of the NPs, but in the absence of any other control experiments it cannot be ruled out that the increased uptake is the indirect result of the altered NP surface on unspecific binding.

4.3.1.3. Micelles. In a series of studies, micelles formed from PEG-*b*-poly(propylene oxide) block copolymers were used to deliver anti-cancer drugs or fluorescent markers into rhabdomyosarcoma (Rh30) or murine mammary tumor (4T1) cells and conjugation of gluconic acid at the C1 position to the PEG chains was shown to result in enhanced cellular uptake of the micelles and increased cytotoxicity.[174–176] Unlike conjugation with gluconic acid, conjugation with galactose yielded uptake and cytotoxicity results which were similar to those found with non-glycoconjugated micelles,[174] which was suggested as evidence for successful GLUT1 targeting, since GLUT1 has a 10-fold lower affinity for galactose than for glucose.[72] On the other hand, glucose deprivation of Rh30 cells for 6 hours prior to incubation with micelles yielded contradictory results – higher intracellular drug release by glucose-conjugated micelles was observed, but also some increase of drug release by non-glycoconjugated micelles, and no effect of glucose deprivation on cytotoxicity was found.[175] Moreover, it has to be noted that glycoconjugation resulted in significant changes to the micellar properties, including significant aggregation, as evidenced by a significantly increased hydrodynamic size (from 17 nm to 200–400 nm), and in some cases a change of the surface charge from positive to negative values, which would be expected to affect unspecific cellular uptake. In particular, the critical micelle concentration of glucose-conjugated copolymers is significantly reduced compared to non-conjugated or galactose-conjugated copolymers, which raises serious doubts about the conclusion of successful GLUT1 targeting. Similarly, conjugation of gluconic acid to the PEG chains of NPs composed of amorphous TiO_2 and PEG-*b*-poly(propylene oxide) block copolymer resulted in a two-fold increase of cellular uptake and significantly enhanced sonodynamic therapy efficacy in 2D and 3D Rh30 cell cultures when compared to non-glycoconjugated NPs.[177] *In vivo* studies further demonstrated faster and more targeted tumour localisation of the glycoconjugated NPs. However, although these effects may result from interaction of the glucose derivative with GLUT1, which is overexpressed in Rh30 cells, other effects, such as NP size or surface charge, cannot be ruled out, especially in light of the results for micelles formed from the same block copolymers, since the effects of glycoconjugation on these parameters were not investigated and no GLUT inhibition studies were reported.

In a similar approach, PEG-poly(ε-caprolactone) block polymeric micelles were investigated as carriers of hydrophobic drug molecules or superparamagnetic iron oxide NPs (SPIONs) for targeted MRI contrast agents. Uptake of 36 nm micelles containing SPIONs into prostate cancer (PC-3) cells was greatly enhanced upon conjugation of glucosamine at the C2 amine group, by a factor of 5 to 27 depending on micelle concentrations, Fig. 6b.[92] Likewise, glucosamine conjugation increased the uptake of 22 nm micelles carrying doxorubicin by up to 100% for GLUT1-overexpressing Hep-G2, MCF-7 and PC-3 cancer cells, whilst showing no effect on the uptake into L929 cells, which do not overexpress GLUT1.[178] Although the latter observation may suggest successful targeting of GLUT1 in the cancer cells lines and glycoconjugation did not greatly affect micelle size or surface charge, potential effects of altered surface chemistry on non-specific binding or uptake cannot be conclusively ruled out in the absence of appropriate control experiments, such as GLUT1-inhibition or glucose competition assays.

Worm-like block copolymer micelles with 800 nm length and 14 nm diameter showed a significant uptake increase, by a factor of up to 10, into MDA-MB-231 and U87-MG cells and U87-MG 3D-spheroids after conjugation of 6-thioglucose (at the C6 position) to their long PEG-chains.[80] Most interestingly, the uptake increase was found to rise with the degree of glycosylation, but plateaued at a certain level, which the authors suggested to arise from saturation of multivalent targeting. The size of the micelles was not affected by glycoconjugation, but no information was provided regarding surface charge and no other control experiments were undertaken. The uptake and release of the cancer drug paclitaxel from Soluplus® copolymer-based micelles (110 nm diameter) into breast cancer cells has been shown to increase significantly, by a factor of up to 8, upon conjugation of glucose at its C1 to the end of some of the long PEG chains of the Soluplus® copolymer.[179] However, glycoconjugation had also been shown to lead to a slight increase of paclitaxel release from

This journal is © The Royal Society of Chemistry 2026

J. Mater. Chem. B, 2026, **14**, 4874–4902 | **4889**

the micelles in solution, and was not investigated independently under cytosolic conditions. Furthermore, although the micelle surface charge was not affected by the glycoconjugation, in the absence of any other control experiments an unspecific effect due to the surface modification rather than interaction with GLUT receptors cannot be ruled out.

The uptake of micellar lipid NPs consisting of 1-tetradecanol and cholesterol, stabilized by poly(2-oxazoline)s with different degrees of glycosylation and hydrodynamic diameters of 20–40 nm, into PC-3 and MDA-MB-231 cancer cells, which over-express GLUT1, was investigated in the absence and presence of excess glucose.[180] For most of these NPs, no increased uptake was found compared to non-glycosylated NPs, and no suppression of uptake by excess glucose was observed, making it likely that non-specific interactions dominate NP binding to the cells.

Nanodiscs (NDs, diameter 50 nm), formed from a mixture of phospholipids, cholesterol and PEG lipids, were modified by the addition of a peptide–glucose (C1) conjugate to the end of the long PEG chains to target GLUT1-mediated transcytosis across the BBB.[181] This resulted in a significant increase (by a factor of 3) of ND uptake into BCECs (bEnd.3) and a minor increase ($\sim$50%) of uptake into U87 glioma cells, which have lower GLUT1 expression,[182] when compared to NDs carrying no peptide or a similar non-glycoconjugated peptide. The increased uptake of the glycoconjugated NDs was further confirmed in 3D models, *in vivo* studies and cytotoxicity results using paclitaxel carrying NDs. Glycoconjugation did not result in any changes of the size, morphology or surface charge of the NDs, which suggested that the increased uptake may result from interaction with GLUT1. On the other hand, the presence of 0.55 M glucose reduced the uptake of the glycoconjugated NDs into bEnd.3 cells only by 25%,[183] which raises some doubts on that suggestion, since this concentration is several orders of magnitude higher than needed for complete blocking of GLUT1,[134] although it is possible that such an extremely high concentration of glucose had other secondary effects, creating a hypertonic environment leading to modification of the cell surface and activation of stress pathways,[184] which may affect ND uptake in different ways.

4.3.1.4. Vesicles. Phospholipid/cholesterol liposomes (LIPs) of 100–120 nm diameter were modified using glucose-cholesterol ligands with 17–26 bonds between the cholesterol and glucose moieties (conjugated at the C6 position) and an increase of uptake into bEnd.3 or glioma cells (C6) was observed compared to the same LIPs not carrying a targeting ligand.[185,186] Dual targeting using glucose and RGD-peptide or biotin ligands showed larger and synergistic effects, which were partly undone by the addition of excess glucose. However, although glycoconjugation did not lead to a significant change of the size or surface charge of the LIPs, the minor changes of NP uptake by adding excess glucose were small and barely or not statistically significant, possibly because of the removal of excess glucose during cell incubation with LIPs, and no direct control experiments for targeting by the glucose cholesterol alone were undertaken, so it is difficult to draw definitive conclusions on GLUT targeting from those observations.

Similarly, glucose was covalently linked (at C6) to LIPs using PEG linkers of varying length, with a minimum length of 30 bonds between the cholesterol and glucose moieties, and transfer through a BBB model consisting of BCECs and astrocytes was found to increase by a factor of approximately 8, compared to similar LIPs without the PEG-glucose ligands.[187] However, it has to be noted that the size of the LIPs with PEG-glucose ligands was significantly smaller (80–100 nm) than that of the control LIPs (158 nm) and that their surface charge was significantly less negative, which could be expected to increase their interaction with the negatively charged plasma membrane. No further control experiments were undertaken. In a similar approach, 125 nm LIPs were modified using glucose bound at C1 by a long PEG-linker to the phospholipid which significantly increased transfer through a BBB model consisting of bEnd.3 cells and subsequent uptake by GL-261 glioma cells.[188] Although size and surface charge of the LIPs were not greatly affected by the glucose modification, in the absence of further control experiments an indirect effect on unspecific cell uptake cannot be ruled out.

4.3.2. Studies with GLUT targeting control experiments. Many of the studies using relatively long linkers between the NP and the glucose moiety described so far did suggest successful GLUT targeting but could not provide conclusive evidence for this effect. However, there have been a number of reports which did succeed in making this conclusion.

4.3.2.1. Inorganic nanoparticles. Gold and silica NPs (11 and $\sim$100 nm diameter, respectively) with a polydopamine (PDA)/PEG coating were shown to be taken up into bEnd.3 cells.[189] Upon glucose conjugation to the PEG capping agent ($\sim$100 bonds) at carbon C6 of glucose, a minor increase of cellular uptake of $\sim$40% was observed for both core materials. It cannot be ruled out that there are some minor contributions from unspecific binding of the NPs to the cell membrane due to the capping layer modification, which resulted in a minor shift of the zeta-potential. However, application of the GLUT1 inhibitor phloretin decreased the uptake of the glucose conjugated AuNPs to the level of the non-glucose conjugated ones but did not affect the uptake of the latter ones, suggesting successful GLUT1 targeting, even if the GLUT1-facilitated NP uptake is only small compared to the unspecific uptake. *In vivo* experiments with these NPs, as well as polymeric NPs with the same PDA/PEG coating, further confirmed the minor uptake increase upon glucose conjugation.

Gold nanoparticles (20 nm diameter) with a mixed PEG/polyion-PEG coating containing small RNA showed an uptake increase into MDA-MB-231 cancer cell spheroids by up to 70% upon conjugation of glucose at C6 to the ends of the polyion-PEGligands.[113] This uptake increase was fully eliminated upon treatment with the GLUT1 inhibitor phloretin, which suggests the involvement of GLUT1 in the increased NP uptake. Targeting by glycoconjugation was also seen in *in vivo* experiments. However, the uptake increase is smaller than the unspecific uptake, and in the absence of experiments testing the effect of phloretin on the unspecific uptake of non-glycoconjugated NPs, it cannot be fully ruled out that the different properties of the capping layer may have affected the unspecific uptake NP
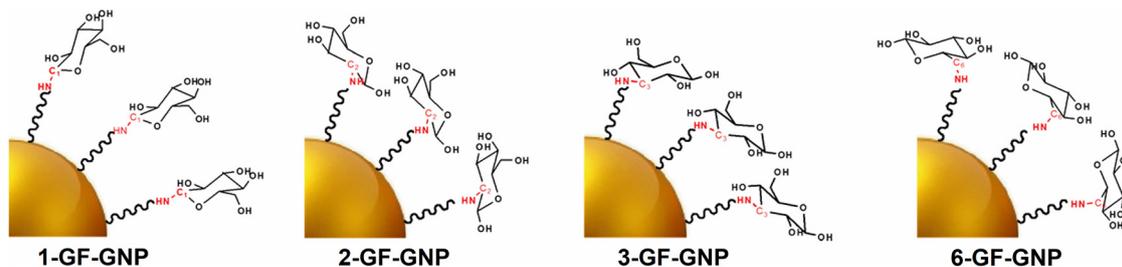
4890 | *J. Mater. Chem. B*, 2026, **14**, 4874–4902

This journal is © The Royal Society of Chemistry 2026

Fig. 9 Schematic diagram of the four glucose-functionalised AuNPs (GF-GNP) used in ref. 78, which differ only in the glucose conjugation site (C1, C2, C3 and C6); the linker is a thio-PEG with 8 repeat units. Adapted from ref. 78 with permission from the American Chemical Society, copyright 2016.

uptake into cells, even if size and surface charge were not affected by glycoconjugation.

One of the most comprehensive series of studies showed conclusively that 20 nm AuNPs can be directed to GLUT1 over-expressing cells by conjugating them with glucosamine *via* a thio-PEG linker (8 repeat units), bound to C2 of glucosamine by an amide bond. Most interestingly, AuNPs conjugated to glucose-C1, C3 or C6 by an amide bond and the same thio-PEG-linker (Fig. 9 shows the structures of the four distinct glucose conjugated AuNPs), which have the same physico-chemical characteristics, were used as control NPs, all of which showed significantly lower uptake into A431 cancer cells (factor 3–5).[78] This observation correlates with the known properties of the glucose binding site in GLUT1, see Fig. 3, which on its own is a very strong indication of GLUT1 targeting. A linear correlation of AuNP uptake with the level of GLUT1 expression was found when comparing four cell lines (cancer cells A431, A549 and LNcaP and 3T3 fibroblast cells), but only for the AuNPs bound to glucose C2, not for the

much smaller uptake of AuNPs linked to C1 (Fig. 10).[88] Competition with excess glucose resulted in significantly lower uptake of the AuNPs bound to glucose C2 into A431 cells, but had only a minor effect on the smaller uptake into 3T3 cells with much lower GLUT1 expression.[78] Pre-incubation with GLUT1 inhibitor Cyt-B was shown to significantly inhibit the uptake of the AuNPs bound to glucose C2 for those cell lines with high GLUT1 expression, but had no effect on the smaller uptake of AuNPs bound to glucose C1 or for cells with low GLUT1 expression (Fig. 11).[88] Taken together, these results conclusively prove GLUT1-mediated uptake of those AuNPs when conjugated to glucosamine C2. Experiments with different endocytosis inhibitors confirmed clathrin-mediated endocytosis as the main uptake mechanism.[88] In addition, 5 and 20 nm AuNPs conjugated to C2 of glucosamine *via* the same thio-PEG linker were also shown to have significantly higher uptake into exosomes with 114 nm diameter derived from mesenchymal stem cells than AuNPs coated with thio-mPEG.[190] Again, glucose competition and
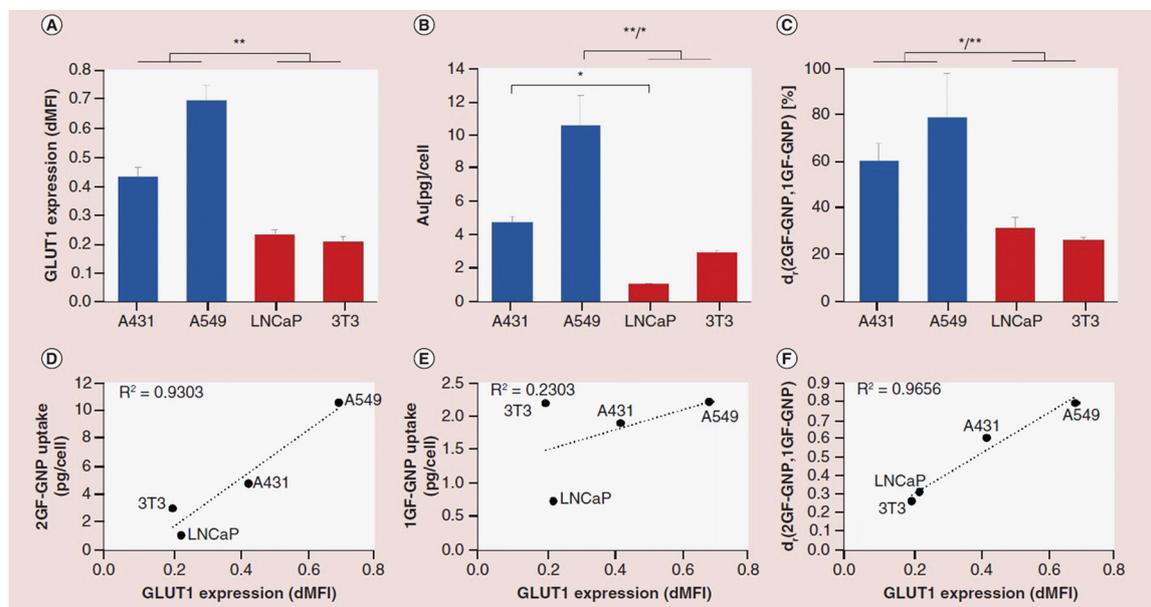
Fig. 10 Comparison of glucose-functionalised AuNP uptake in cell lines with different GLUT1 expression (A431, A549, LNcaP, 3T3). (A) Relative GLUT1 expression in the four cell types. (B) Uptake of AuNPs conjugated to glucose C2 (2GF-GNP) in the various cell lines, measured by FAAS. (C) Relative difference between cellular uptake of 2GF-GNP and AuNPs conjugated to glucose C1 (1GF-GNP), defined as: d_r = 100*(2GF-GNP − 1GF-GNP)/2GF-GNP. (D–F) Correlation between GLUT1 expression and (D) 2GF-GNP uptake, (E) 1GF-GNP uptake and (F) d_r. Reproduced from ref. 88 with permission from Informa UK Limited, trading Taylor & Francis Group, copyright 2018.

This journal is © The Royal Society of Chemistry 2026

J. Mater. Chem. B, 2026, **14**, 4874–4902 | **4891**
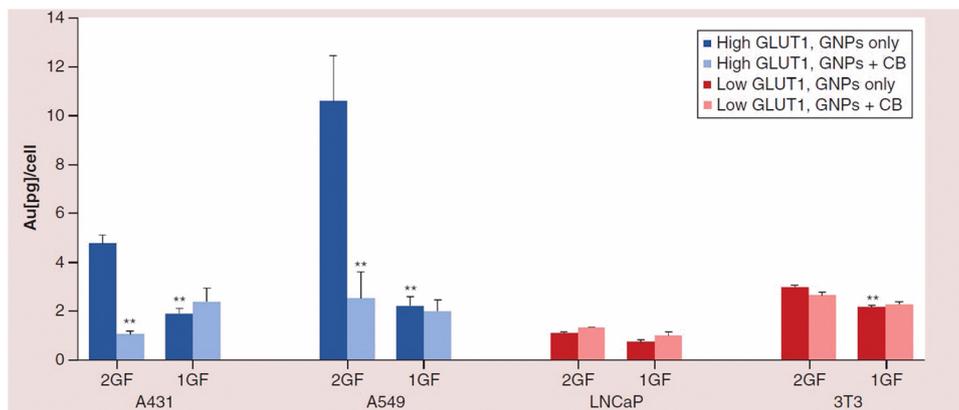
Fig. 11 Effect of GLUT1 inhibitor cytochalasin B (CB) on the uptake of glucose-functionalised AuNPs (GNPs) conjugated to glucose C1 (1GF) or C2 (2GF) in cell lines with different GLUT1 expression, measured by FAAS. Blue bars indicate high GLUT-1-expressing cells (A431, A549), red bars indicate low GLUT-1-expressing cells (LNCaP, 3T3). Reproduced from ref. 88 with permission from Informa UK Limited, trading Taylor & Francis Group, copyright 2018.

GLUT1 inhibition by Cyt-B resulted in a significant reduction of cell uptake, to a level similar to the thio-mPEG coated AuNPs, proving the involvement of GLUT1 in NP uptake.

Ovalbumin coated Gd_2O_3 NPs (21 nm hydrodynamic diameter) showed significantly increased uptake into mouse bone marrow-derived dendritic cells, which overexpress GLUT1, after conjugation of glucose *via* a long linker (1k-PEG-maleimide-mercaptoundecanoic acid, bound to C2 of glucose), when compared to non-glycoconjugated NPs.[44] Phloretin decreased the uptake of the glycoconjugated NPs to the level of the non-glycoconjugated ones, but did not affect the uptake of the latter ones, which is a strong indication of successful targeting of GLUT1. *In vivo* experiments also showed significantly decreased tumour growth and increased survival rates due to the triggering of immune responses upon glycoconjugation of Gd_2O_3@ovalbumin NPs.

3 nm CdTe QDs capped with lipoic acid, lysine and 9-poly(arginine), resulting in a hydrodynamic diameter of 130 nm, showed increased uptake into HepG2 cancer cells upon conjugation of glucosamine at the C2 amine group *via* a 2k-PEG linker, both in absence and in presence of a siRNA payload.[191] Glycoconjugation increased the hydrodynamic diameter and changed the surface charge from slightly positive to neutral. However, a range of observations confirmed specific binding of the glycoconjugated QDs to GLUT1, which is overexpressed in HepG2 cells: (i) minimal uptake of the glycoconjugated QDs into U87-MG cells, known to have very low GLUT1 expression; (ii) significantly increased uptake of these QDs into HepG2 cells under hypoxic conditions, which increases GLUT1 expression; and (iii) significant blocking of NP uptake after pretreatment with free glucosamine. *In vivo* experiments further supported successful targeting of tumour cells. Similarly, 8 nm CdSe/ZnS core–shell QDs showed strongly increased uptake into differentiated C2C12 muscle cells, which overexpress GLUT4, upon conjugation of glucose at C1 *via* a long linker (25 bonds).[192] The addition of insulin, which stimulates the translocation of GLUT4 to the cell membrane, further increased QD uptake, whereas competition with excess 2-deoxyglucose significantly reduced the

uptake, which strongly supports specific binding of the glycoconjugated QDs to GLUT4.

Luminescent $CaMgSiO_3NPs$ (20–30 nm), doped with various metal and rare earth elements and coated with PAMAM dendrimers, were conjugated with 2-deoxy-glucose; it was found that in the presence of excess glucose uptake of these NPs into WEHI-164 fibrosarcoma cells was reduced by a factor of three, strongly suggesting the involvement of GLUT receptors that are blocked by glucose competition.[193] This was further supported by the observation that cancer cells had much lower viability upon incubation with these glycoconjugated NPs than non-cancerous (3T3) cells, and that the viability of the cancer cells, but not that of the non-cancerous cells, was slightly increased in the presence of glucose. *In vivo* testing also confirmed selective tumour cell targeting and decreased tumour growth.

4.3.2.2. Polymeric nanoparticles. PAMAM dendrimer nanoconjugates (12–13 nm and 40–43 nm, respectively), functionalised with different anticancer drugs, were reported to have significantly increased uptake into HepG2 or MCF-7 cancer cells after conjugation of glucose to a long PEG linker at carbon C2, with significantly lower uptake of the glycoconjugated NPs into non-cancerous L02 cells with low GLUT1 expression.[194,195] Pre-incubation with 2.5 mM glucose for 4 hours significantly reduced uptake of the glycoconjugated NPs into the cancer cells, supporting GLUT1-mediated uptake as the primary mechanism of targeted delivery. *In vitro* and *in vivo* experiments further confirmed the increased inhibitory effect of drug-loaded NPs after conjugation with glucose. GLUT1-mediated uptake was also shown for similar13 nm PAMAM dendrimers conjugated with doxorubicin, showing increased cytotoxicity upon conjugation with glucose that was largely reversed upon application of GLUT1 inhibitors.[196]

240 nm NPs formed from branched glucose-PLGA polymer (Glu-PLGA) were investigated as cancer drug carriers and it was shown that in glucose-free conditions the uptake of Glu-PLGA NPs into Hep-2 cancer cells was more than three times higher

than that of non-glycoconjugated PLGA NPs of the same size and surface charge.[90] During synthesis of branched glucose-PLGA polymers, polymerization can start at any of the glucose hydroxyl groups, which is why they formally often are shown with PLGA chains starting from all five glucose hydroxyl groups; this most likely would result in a polymer that could not bind to the GLUT1 binding site, as discussed above. However, it is well known that the branching ratio of Glu-PLGA polymers is normally much smaller,[197] especially for polymers with lower MW as used here, so that it seems highly likely that a significant fraction of the glucose moieties are at the end of a single (long) PLGA chain, and thus should be able to bind to GLUT1, unless conjugation is to glucose-C3, see Fig. 3. In agreement with this expectation, the presence of 25 mM glucose reduced the uptake of the Glu-PLGA NPs to the level of the PLGA NPs but had almost no effect on the uptake of the latter, see Fig. 5b, which provides convincing evidence for the involvement of GLUT1 in the uptake of the Glu-PLGA NPs.

A significant effect was also found for paclitaxel-loaded PEG-PTMC polymeric NPs with a diameter of 71 nm, for which an increase of uptake into RG-2 glioma cells and transport through a BBB model (bEnd.3 cells) by a factor of approximately 2 was found upon conjugation of glucosamine via the PEG constituent ($\sim$60 bonds).[111] Competition with glucose as well as the addition of the GLUT1 inhibitor Cyt-B reduced uptake to almost the level of non-glycoconjugated NPs, which confirms the involvement of GLUT1 in the enhanced NP uptake. These results were complemented by in vitro experiments confirming the higher cytotoxicity of the glycoconjugated NPs[198] and their deeper permeation into 3D spheroids, and by in vivo experiments which showed the successful transport of the glycoconjugated NPs into the brain of glioma-bearing mice, whereas essentially no NPs could be detected without glycoconjugation.

Glycoconjugated PDA-NPs were developed as a pH- and photothermal-responsive targeted drug delivery system by covalent attachment of glucosamine(Glc-NH$_2$) at its C2 amine group or 3-amino-1-diethylene glycol-α-D-glucopyranoside (Glc-DEG-NH$_2$) at C1.[199] In vitro cell viability studies confirmed delivery of the anticancer drug bortezomib (BTZ) into MDA-MB-231 and MCF-10A cells by both glycoconjugated PDA-NPs, whereas BTZ-loaded non-glycoconjugated PDA-NPs did not affect cell viability. The effect was significantly more pronounced for the GLUT1-overexpressing MDA-MB-231 cancer cells than the non-cancerous MCF-10A cells and was almost completely inhibited by adding excess glucose (10 mM). NP uptake experiments on MDA-MB-231 cells showed an uptake increase by a factor of 35 and 46 for PDA-NPs conjugated with Glc-NH$_2$ and Glc-DEG-NH$_2$, respectively, compared to non-glycoconjugated PDA-NPs. Uptake of the glycoconjugated PDA-NPs was reduced to the level of uptake of non-glycoconjugated PDA-NPs by GLUT1 inhibitor WZB117 (10 μM), whereas the inhibitor had no effect on the uptake of non-glycoconjugated PDA-NPs; however, it should be noted that cells were incubated with the inhibitor for 24 hours prior to NP incubation, which may cause secondary effects, as discussed above. Overall, these results strongly support the suggestion of GLUT1-mediated uptake, and the usefulness of the glycoconjugated

PDA-NPs was further confirmed by in vivo experiments. The fact that NP uptake and BTZ delivery were found to be higher for PDA-NPs conjugated to Glc-DEG-NH$_2$ than those conjugated to Glc-NH$_2$ could suggest that the additional thin and flexible linker for the former, comprising of 2 ethylene units, compared to the slightly more bulky and rigid PDA polymer strand which constitutes the linker for the latter, enhances its capacity for accessing the glucose binding site in the centre of GLUT1, see Fig. 1; however, this difference may also be due to the reported significantly higher glucose loading when using Glc-DEG-NH$_2$.

100 nm nanocapsules, formed by the polymerisation of N-(3-aminopropyl) methacrylamide around an antibody-siRNA conjugate, were shown to have a threefold higher penetration efficiency through a BBB model consisting of bEnd.3 cells and significantly higher uptake into U87 cancer cells after conjugation of 2-deoxy-glucose to the polymer.[98] While glycoconjugation slightly increased the hydrodynamic diameter of the nanocapsules, it did not alter the surface charge. Crucially, the presence of 20 mM glucose reduced the BBB-model penetration efficiency and cell uptake to the level of the non-glycosylated nanocarriers, which provides strong evidence of the involvement of GLUT1, which is overexpressed in both cell lines.

4.3.2.3. Micelles. In the context of studying drug carrier modifications that allow them to cross the BBB, it was shown that the transport efficiency through a BBB model consisting of BCECs increased by more than a factor of 2 when Pluronic P105 polymeric micelles (25 nm diameter) were modified by the addition of glucose to the end of the polymer at glucose carbon C6.[200] Similarly, the inclusion of a small amount of a modified phospholipid carrying a long PEG-glucose ligand (conjugated at glucose carbon C1) into LIPs of 110 nm diameter caused a more than two-fold increase of uptake into BCECs and an even larger increase of the transport efficiency through a BBB model, compared to LIPs without glycoconjugation.[201] Although glycoconjugation did not affect the surface charge of the micelles and no effect was observed by the conjugation of folic acid to the micelles or an RGD peptide motif to the LIPs, these results on their own might be due to some unspecific binding effects. However, uptake or transport efficiency of the glucose-conjugated particles was significantly reduced by the addition of 0.5–1 mM glucose, a strong indication of the involvement of GLUT1 which is overexpressed in BCECs. These results were further supported by successful in vivo experiments in both studies.

Decorating 30 nm PEG-polyion polymer micelles with glucose via a long PEG linker, see Fig. 12a, resulted in a fourfold increase of uptake into Neuro2a cells transfected with a GLUT1 expressing plasmid; no such increase was seen in cells transfected with a mock plasmid, see Fig. 12b.[40] This uptake increase was found to be independent of the fraction of negative polyions that were functionalised with glucose, at least in the investigated range of 25–50%. Similar PEG-polymer micelles with a diameter of 45 nm and modified polyion chemistries showed a similar increase in uptake into breast cancer cells (MDA-MB-231), as well as a twofold increase in uptake into Caco-2 colon cancer cells and rat brain endothelial cells upon glucose decoration; in both cases,

This journal is © The Royal Society of Chemistry 2026

J. Mater. Chem. B, 2026, **14**, 4874–4902 | **4893**

the degree of glycosylation was varied over a wider range (up to 100%), with increasing glycosylation resulting in measurably larger uptake increase.[110,112] For all of these glycoconjugated micelles, GLUT1 inhibitors completely removed the additional uptake, but did not affect the uptake of non-glycoconjugated micelles, see Fig. 12c, which provides convincing evidence of successful GLUT1 targeting by this glucose conjugation method. As a further control, the additional uptake was observed only when glucose was linked at its C6 carbon, but not when it was linked at the C3 carbon, see Fig. 12b,[40] in line with the expectations discussed above (Fig. 3). These *in vitro* results were accompanied by successful *in vivo* results showing transfer of the glycoconjugated micelles across the BBB and subsequent release of the drug payload.

PEG/poly(glutamic acid) block copolymers, self-assembled into 30 nm micelles by complex formation with the cancer drug cisplatin, were found to have higher *in vitro* cytotoxicity against multicellular spheroids of GLUT1-rich OSC-19 cancer cells after glucose conjugation at C6 at the end of some of the long PEG

chains, which did not affect size or surface charge of the micelles.[119] In comparison, the cytotoxicity of these micelles was found to be independent of glycoconjugation for U87-MG cells which express GLUT1 to much lower extent. Moreover, knocking down GLUT1 in OSC-19 cells resulted in significantly lower and glycoconjugation-independent cytotoxicity; although indirect effects of the intracellular glucose starvation in the GLUT1-knockdown cells cannot be ruled out,[104–106] as discussed above, this suggests the involvement of GLUT1 in the uptake enhancement by glucose conjugation. *In vivo* OSC-19 tumour model investigations also demonstrated superior uptake of the glycoconjugated micelles, with GLUT1-inhibitor STF-31 or excess glucose injections reducing uptake of glycoconjugated micelles whilst uptake of the non-glycoconjugated micelles was not affected. Most interestingly, micelles with less glucose on their surface showed higher antitumour activity in these *in vivo* experiments, whereas no significant effect of varying the extent of glucose conjugation were seen in the *in vitro* experiments. This was shown to arise from a more rapid clearance of the
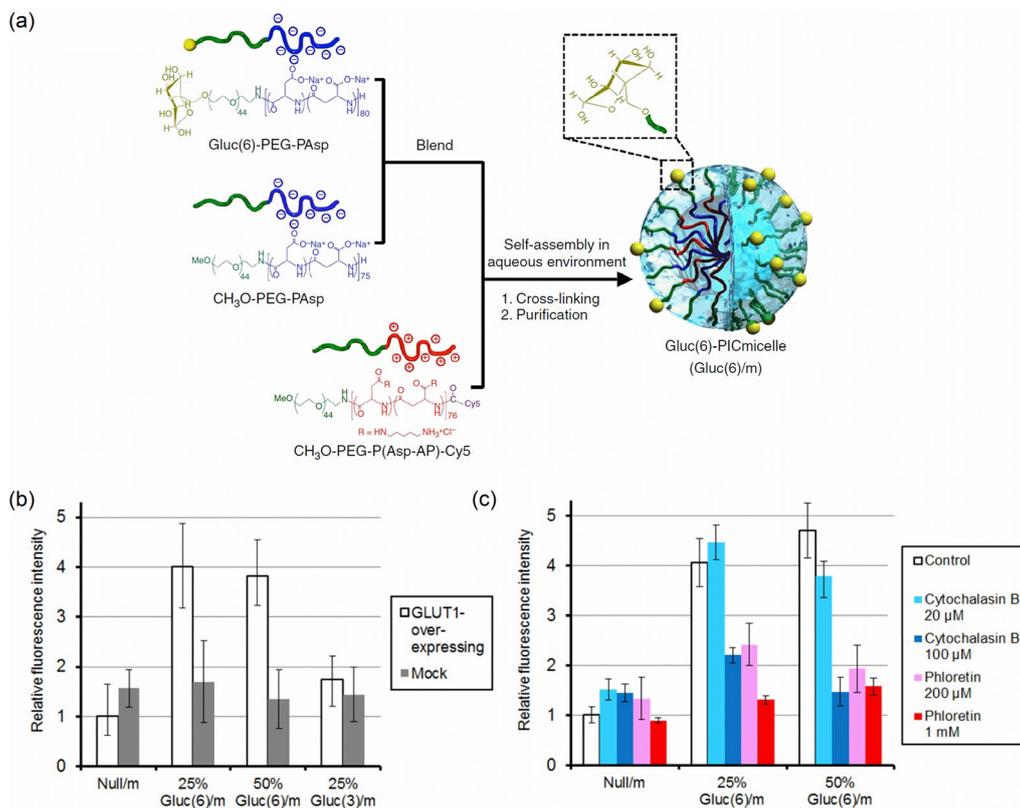
Fig. 12 Cellular uptake of glucose-decorated PEG-polyion polymer micelles. (a) Methoxy- and glucose-conjugated PEG-poly(α,β-aspartic acid) block copolymers (CH$_3$O-PEG-PAsp and Gluc(6)-PEG-PAsp, respectively) were mixed at different ratios. Oppositely charged methoxy-PEG-poly([5-aminopentyl]-α,β-aspartamide) block copolymer, labelled with fluorescent dye Cy5, (CH$_3$O-PEG-P(Asp-AP)-Cy5) was added and the resulting micelles were stabilised by crosslinking with 1-ethyl-3-(3-dimethylaminopropyl) carbodiimide. (b and c) Uptake of PEG-polyion polymer micelles into Neuro2a cells co-transfected with GLUT1 expressing plasmid (GLUT1-overexpressing) or mock plasmid: (b) Uptake of micelles without glucose decoration (null/m) and micelles formed using glucose/methoxy-conjugated PEG-PAsp at ratios of 25/75 or 50/50. Gluc(6) indicates glucose conjugation at carbon C6, as shown in (a), Gluc(3) indicates conjugation at C3. (c) Effect of GLUT1 inhibitors on the uptake of micelles without glucose decoration (null/m) and micelles formed using glucose (C6)/methoxy-conjugated PEG-PAsp at ratios of 25/75 or 50/50 into GLUT1-overexpressing cells. Relative uptake was quantified using the fluorescence of cell suspensions after incubation with micelles, normalized to the fluorescence of GLUT1-overexpressing cells treated with null/m in the absence of inhibitors. Reproduced from ref. 40 with permission from Springer Nature, copyright 2017.

4894 | *J. Mater. Chem. B*, 2026, **14**, 4874–4902

This journal is © The Royal Society of Chemistry 2026

glucose-rich micelles from the bloodstream into the liver, emphasizing the complexity of the interplay between opposing factors in practical applications of nanomedicines.

4.3.2.4. Vesicles. In a similar approach, ∼100 nm phospholipid/PEG vesicles containing polyaspartic acid/PEI/siRNA as the payload showed over tenfold higher uptake into C6/TR cancer cells and double the transport efficiency across a BBB model consisting of bEND.3 cells when the end of the 2k-PEG chain was conjugated to glucosamine (at C2).[202] Although no information on the size or surface charge of the non-glycoconjugated NPs was given, the addition of phlorizin, a GLUT1 inhibitor, reduced the uptake and BBB model transport of the glycoconjugated NPs almost to the level of the non-glycoconjugated NPs, while having no effect on the non-glycoconjugated controls. This strongly confirms the involvement of GLUT1 in mediating cellular uptake. *In vivo* experiments further supported this conclusion.

The replacement of cholesterol by the structurally similar glucose-terminated ginsenoside Rg-3 (glucose conjugated at C1) for the formation of phospholipid–liposomes resulted in 2–3 times higher uptake into C6, BCEC and HUVEC cells, all of which overexpress GLUT1, and a similar increase of the transport of these LIPs across a BBB model consisting of BCEC cells.[203] Although this was shown to partly arise from the smaller size of the glucose-terminated LIPs (66 *vs.* 126 nm), a measurable uptake increase was also observed when larger glucose-terminated LIPs were incubated with C6 cells. GLUT1-mediated uptake as a contributing effect was confirmed by a significant decrease of uptake of the glucose-terminated LIPs by all three cell lines in the presence of excess glucose or GLUT1-inhibitors, whereas there was no effect for the uptake of non-glycoconjugated LIPs.

125 nm liposomes were conjugated to the C2 amine group of glucosamine *via* a long PEG spacer, which caused significantly greater uptake into cancer cell lines with high metabolic activity, most likely caused by high GLUT1 expression (A431, A549, B16,

4T1), compared to non-conjugated controls.[204] In contrast, cells with low metabolic activity (LNCaP, 3T3 fibroblasts) exhibited no significant difference in uptake between glycoconjugated and non-conjugated liposomes. Competitive inhibition studies using Cyt-B and excess glucose further supported a GLUT1-mediated uptake mechanism, with reduced uptake of glucose-conjugated liposomes observed under these conditions. These findings were reaffirmed in a follow-up study, which consistently demonstrated preferential uptake of glucose-coated liposomes by high GLUT1-expressing cancer cells (A431, 4T1, PC-3, MDA-MB-231), compared to non-glycoconjugated or mannose-conjugated liposomes.[140] The latter showed slightly increased cellular uptake compared to non-conjugated liposomes, but much lower uptake than glucose-conjugated ones, aligning with the tenfold lower affinity of mannose for GLUT1 when compared to glucose.[72]

4.3.3. Conclusions. The literature summarised in the preceding section shows that NPs can be targeted towards GLUT-overexpressing cells using a glucose ligand, provided that a linker longer than 15 bonds is used to tether it to the NP. This is in agreement with the conclusion of Section 2 that glucose can only reach the central binding site if the tether is longer than 20 Å, since the NP is not able to significantly penetrate into the narrow channel leading from the receptor surface to the binding site. The results validate the general approach of GLUT targeting by glucose-conjugated NPs, although it needs to be stressed that not all studies investigating a longer linker have conclusively proven that the increased uptake of glucose-conjugated NPs is due to interaction with GLUT.

4.4. Summary - design principles for GLUT-targeting nanoparticles

The evidence reviewed above converges on several design parameters that govern the effective construction of GLUT-targeting NPs, as summarised in Table 1.

Our literature review shows that there is no evidence that direct conjugation of glucose to a NP or even the use of a linker

Table 1 Summary of evidence-informed design principles for glucose transporter (GLUT)-targeting nanoparticles

Design parameter	Guidance	Strength of evidence[a]	Relevant references
Tether length	GLUT structure shows that a minimum of 15–20 bonds are required to permit access of glucose to the central GLUT binding site. This is supported by the observation that there is no evidence of GLUT-specific uptake in NPs with glucose bound directly or *via* a shorter linker	Strong	52, 58 and 59
Tether chemistry	Based on small molecule studies, both hydrophilic and hydrophobic elements on the tether are expected to strengthen binding, although hydrophobic tethers my increase non-selective uptake. No evidence available from NP studies.	Moderate	77, 81–83, 85 and 86
Glucose conjugation site	C1, C2 or C6 conjugation preserves sufficient hydrogen-bonding interactions for GLUT recognition, although conjugation *via* C1 or C6 must include a hydrogen bond acceptor; evidenced by many small molecule and some NP studies. C3 is unlikely to be a suitable conjugation site, whereas the suitability of C4 conjugation remains unclear.	Strong	39, 40, 47, 75, 78, 79 and 88
Ligand density	A larger number of glucose ligands is expected to increase the NP's affinity to GLUT or even allow for multivalent targeting. On the other hand, increased ligand density may reduce the affinity due to steric hindrance, particularly for tethers with a length close to the minimum (see above). Investigation of this effect remains highly limited.	Weak	40, 80, 110, 112 and 119

[a] Strength of evidence defined as: strong – multiple independent studies with consistent findings and structural/mechanistic corroboration; moderate – several studies with convergent trends but systems-dependent variability and/or incomplete mechanistic validation; weak – limited number of studies, poor quantification or inconsistent reporting across the system.

This journal is © The Royal Society of Chemistry 2026

J. Mater. Chem. B, 2026, **14**, 4874–4902 | **4895**

that is shorter than 15–20 bonds allows targeting of these NPs to GLUT-overexpressing cells, at least for NPs that are larger than ~ 2 nm. This is in agreement with the predictions based on the 3D structure of GLUTs outlined in Section 2, showing that the glucose binding site is deep inside the receptor and can only be reached *via* a narrow channel (Fig. 1). On the other hand, there is clear evidence that NPs conjugated to glucose *via* a longer linker can be successfully targeted to GLUT. Although there are many studies using appropriate long linkers, these often lack essential controls such as GLUT inhibition or competition assays and findings must therefore be interpreted with caution. The studies summarised in Section 4.3.2, however, did include appropriate validation and controls.

In most cases PEG chains were used to provide the necessary reach and flexibility, but other hydrophilic linkers such as PAMAM, PLGA or PDA spacers have also proven effective (SI). It is unclear at the present moment to what extent any interactions between the tether and the residues lining the channel leading to the glucose binding site contribute to the binding affinity, since no data are available to answer this question. No hydrophobic tethers have been investigated.

The carbon position used for glucose conjugation is an important factor in GLUT recognition. We have found numerous examples of successful GLUT targeting NPs with glucose conjugated at C1, C2 or C6. All examples using conjugation to C1 or C6 involve an ether bond, *i.e.* they retain the hydroxyl oxygen. The need for a hydrogen bond acceptor at these positions, which already was postulated based on GLUT binding studies of small molecules (Section 2.3), is highlighted by the lack of uptake of NPs where the hydroxyl oxygen at C1 or C6 has been replaced by nitrogen as part of a peptide bond to the linker.[78] Conversely, conjugation to C2 seems to be more flexible, in line with the expectations based on small molecule studies; most examples found here use a peptide bond, often using the easily available 2-amino-2-deoxy-D-glucose (glucosamine) and standard carbodiimide chemistry. The question whether conjugation at C3 or C4 is possible remains open, although the general considerations discussed in Section 2.3 seem to rule out GLUT recognition after glucose conjugation at C3, but do not rule out conjugation at C4, provided that a hydrogen bond acceptor is bound to the carbon.

On the other hand, the question of the ligand density on the NP surface has not been widely studied. As described in Section 2.3, a dense layer of glucose-bearing ligands may result in steric hindrance, impeding access of the glucose moiety to the glucose binding site. Unfortunately, most of the literature discussed here did not quantify the number of glucose bound to each NP at all and even less studies investigated the effect of varying the ligand density on NP uptake or toxicity. The few studies that did so found either no effect[40,119] or increased uptake with increasing glucose density.[80,110,112] However, all of these studies investigated glucose bound at the end of very long PEG tethers on polymeric or micellar NPs with relatively low ligand density (typically less than 0.1 glucose per nm², which is much lower than the density of ~ 5 ligands per nm² which can be achieved with shorter PEG ligands on AuNP surfaces[205]). The length of the tether and the low ligand density rule out

significant steric hindrance, so that this question remains open for now; it will be interesting to see more detailed work on this in the future.

In summary, successful GLUT recognition appears to depend on presenting glucose at a sufficient distance from the NP surface and selecting a conjugation site that preserves key hydrogen-bonding interactions. Long, flexible linkers, such as PEG together with C2 or ether-linked C1/C6 attachment currently represent the most promising design features for glucose–NP conjugates.

5. Conclusion

The literature reports a wide range of NPs, from solid inorganic metal clusters to liposomal, micellar or polymeric formulations that have been modified by glucose conjugation for targeting GLUTs. Most of these were reported to have increased cellular uptake compared to their non-glycoconjugated equivalents. However, many of these studies fail to consider that glycoconjugation also affects other NP properties which are well-known to influence cellular uptake, most notably the NP surface charge. Consequently, increased uptake alone cannot be taken as definitive evidence of GLUT-mediated targeting, as surface modification may enhance non-specific cellular uptake without achieving the desired cell specificity. Robust confirmation of GLUT involvement requires the use of appropriate controls, such as glucose competition, GLUT inhibition, or gene silencing approaches.

This review supports the predictions derived from GLUT structural models. Direct conjugation of glucose to solid NPs or the use of short linkers has not provided convincing evidence of true GLUT-mediated uptake, whereas long and flexible linkers, combined with suitable attachment chemistry, have repeatedly validated the glucose-conjugated blueprint, in agreement with the known GLUT binding pocket architecture. This demonstrates that glucose functionalisation is not only conceptually sound but, when applied with structural and methodological precision, genuinely works as a route to achieve selective transporter-mediated nanomedicine delivery in cancer cells or blood brain barrier delivery applications.

The path towards clinical applications of glucose-conjugated NPs will need to carefully consider the conditions that are being targeted. Due to the omnipresence of GLUTs, only cells with sufficient overexpression of glucose transporters can be targeted specifically without greatly affecting other cells. This includes many cancer cell types due to the Warburg effect, *i.e.* the enhanced requirement of glucose for the aerobic glycolysis employed by those cells.[37–39] Although the most widely overexpressed GLUT isoform in cancer cells is GLUT1, some cancers overexpress other isoforms, which may be better targeted by other hexoses, or are characterized by only small overexpression levels. Thus, glucose-conjugated NPs may not be suitable for all conditions. Similarly, it is well documented that conditions like inflammation or infection lead to increased uptake of glucose, which is one of the major drawbacks of ¹⁸F-FDG tomography.[206] Thus, care will have to be taken to avoid off-target effects,

4896 | *J. Mater. Chem. B*, 2026, **14**, 4874–4902

This journal is © The Royal Society of Chemistry 2026

although preliminary results suggest that glucose-conjugated NPs, unlike ^{18}F-FDG, do not target inflammatory tissue.[78]

Progress in this field will depend on consistent use of rigorous validation strategies, but the main design rules are now clear, requiring careful selection of linker length as well as conjugation site and chemistry to achieve transporter-mediated delivery. We hope that future studies will build on the principles outlined in this review to advance glucose-targeted nanoparticle research and ultimately further our progress towards transporter-targeted treatment strategies.

Conflicts of interest

The authors declare no conflicts of interest.

Data availability

Data sharing is not applicable to this article as no new data were created or analyzed. The Supporting Information includes a comprehensive summary table of all the literature reviewed (Table S1), detailing nanoparticle characteristics, linker chemistry, glucose conjugation site, uptake quantification methods, experimental models, and reported control strategies (including glucose competition and inhibitor studies).

Supplementary information (SI) is available. See DOI: https://doi.org/10.1039/d5tb02390d.

Acknowledgements

References

1 A. C. Anselmo and S. Mitragotri, *Bioeng. Transl. Med.*, 2019, **4**, e10143, DOI: 10.1002/btm2.10143.

2 R. van der Meel, E. Sulheim, Y. Shi, F. Kiessling, W. J. M. Mulder and T. Lammers, *Nat. Nanotechnol.*, 2019, **14**, 1007–1017, DOI: 10.1038/s41565-019-0567-y.

3 M. J. Mitchell, M. M. Billingsley, R. M. Haley, M. E. Wechsler, N. A. Peppas and R. Laner, *Nat. Rev. Drug Discovery*, 2021, **20**, 101–124, DOI: 10.1038/s41573-020-0090-8.

4 S. N. Bhatia, X. Chen, M. A. Dobrovolskaia and T. Lammers, *Nat. Rev. Cancer*, 2022, **22**, 550–556, DOI: 10.1038/s41568-022-00496-9.

5 D. Fan, Y. Cao, M. Cao, Y. Wang, Y. Cao and T. Gong, *Signal Transduction Targeted Ther.*, 2023, **8**, 293, DOI: 10.1038/s41392-023-01536-y.

6 C. Wang and S. Zhang, *ACS Appl. Nano Mater.*, 2023, **6**, 22594–22610, DOI: 10.1021/acsanm.3c04487.

7 Q. Zhou, J. Xiang, N. Qiu, Y. Wang, Y. Piao, S. Shao, J. Tang, Z. Zhou and Y. Shen, *Chem. Rev.*, 2023, **123**, 10920–10989, DOI: 10.1021/acs.chemrev.3c00062.

8 S. Bandaru, M. Palanivel, M. Ravipati, W.-Y. Wu, S. Zahid, S. S. Halkarni, G. K. Dalapati, K. K. Ghosh, B. Gulyás, P. Padmanabhan and S. Chakrabortty, *ACS Omega*, 2024, **9**, 7452–7462, DOI: 10.1021/acsomega.3c04962.

9 G. Feng, B. Kong, J. Xing and J. Chen, *Clin. Radiol.*, 2014, **69**, 1105–1111, DOI: 10.1016/j.crad.2014.05.112.

10 M. Broadbent, S. J. Chadwick, M. Brust and M. Volk, *ACS Omega*, 2024, **9**, 44846–44859, DOI: 10.1021/acsomega.4c08797.

11 T. Kong, J. Zeng, X. Wang, X. Yang, J. Yang, S. McQuarrie, A. McEwan, W. Roa, J. Chen and J. Z. Xing, *Small*, 2008, **4**, 1537–1543, DOI: 10.1002/smll.200700794.

12 M. A. Beach, U. Nayanathara, Y. Gao, C. Zhang, Y. Xiong, Y. Wang and G. K. Such, *Chem. Rev.*, 2024, **124**, 5505–5616, DOI: 10.1021/acs.chemrev.3c00705.

13 N. R. S. Sibuyi, K. L. Moabelo, A. O. Fadaka, S. Meyer, M. O. Onani, A. M. Madiehe and M. Meyer, *Nanoscale Res. Lett.*, 2021, **16**, 174, DOI: 10.1186/s11671-021-03632-w.

14 X. Zheng, J. Xie, X. Zhang, W. Sun, H. Zhao, Y. Li and C. Wang, *Chin. Chem. Lett.*, 2021, **32**, 243–257, DOI: 10.1016/j.cclet.2020.11.029.

15 A. Bose, D. R. Burman, B. Sikdar and P. Patra, *IET Nano-biotechnol.*, 2021, **15**, 19–27, DOI: 10.1049/nbt2.12018.

16 P. Mi, H. Cabral and K. Kataoka, *Adv. Mater.*, 2020, **32**, 1902604, DOI: 10.1002/adma.201902604.

17 A. Heuer-Jungemann, N. Feliu, I. Bakaimi, M. Hamaly, A. Alkilany, I. Chakraborty, A. Masood, M. F. Casula, A. Kostopoulou, E. Oh, K. Susumu, M. H. Stewart, I. L. Medintz, E. Stratakis, W. J. Parak and A. G. Kanaras, *Chem. Rev.*, 2019, **119**, 4819–4880, DOI: 10.1021/acs.chemrev.8b00733.

18 A. J. Trouiller, S. Hebié, F. el Bahhaj, T. W. Napporn and P. Bertrand, *Eur. J. Med. Chem.*, 2015, **99**, 92–112, DOI: 10.1016/j.ejmech.2015.05.024.

19 M. A. Raheem, M. A. Rahim, I. Gul, X. Zhong, C. Xiao, H. Zhang, J. Wei, Q. He, M. Hassan, C. Y. Zhang, D. Yu, V. Pandey, K. Du, R. Wang, S. Han, Y. Han and P. Qin, *OpenNano*, 2023, **12**, 100152, DOI: 10.1016/j.onano.2023.100152.

20 Y. Zhong, F. Meng, C. Deng and Z. Zhong, *Biomacromolecules*, 2014, **15**, 1955–1969, DOI: 10.1021/bm5003009.

21 A. Ahmad, F. Khan, R. K. Mishra and R. Khan, *J. Med. Chem.*, 2019, **62**, 10475–10496, DOI: 10.1021/acs.jmedchem.9b00511.

22 N. Bertrand, J. Wu, X. Xu, N. Kamaly and O. C. Farokhzad, *Adv. Drug Delivery Rev.*, 2014, **66**, 2–25, DOI: 10.1016/j.addr.2013.11.009.

23 D. Rosenblum, N. Joshi, W. Tao, J. M. Karp and D. Peer, *Nat. Commun.*, 2018, **9**, 1410, DOI: 10.1038/s41467-018-03705-y.

24 S. Mizrahy, A. Gutkin, P. Decuzzi and D. Peer, *J. Drug Targeting*, 2019, **27**, 542–554, DOI: 10.1080/1061186X.2018.1533556.

25 J. Li and K. Kataoka, *J. Am. Chem. Soc.*, 2021, **143**, 538–559, DOI: 10.1021/jacs.0c09029.

26 N. Kaur, P. Popli, N. Tiwary and R. Swami, *J. Controlled Release*, 2023, **355**, 417–433, DOI: 10.1016/j.jconrel.2023.01.032.

27 H. Maeda, K. Tsukigawa and J. Fang, *Microcirculation*, 2016, **23**, 173–182, DOI: 10.1111/micc.12228.

This journal is © The Royal Society of Chemistry 2026

J. Mater. Chem. B, 2026, **14**, 4874–4902 | **4897**

28 Y. Nakamura, A. Mochida, P. L. Choyke and H. Kobayashi, *Bioconjugate Chem.*, 2016, **27**, 2225–2238, DOI: 10.1021/acs.bioconjchem.6b00437.

29 Y. S. Youn and Y. H. Bae, *Adv. Drug Delivery Rev.*, 2018, **130**, 3–11, DOI: 10.1016/j.addr.2018.05.008.

30 Q. Zhou, J. Li, J. Xiang, S. Shao, Z. Zhou, J. Tang and Y. Shen, *Adv. Drug Delivery Rev.*, 2022, **189**, 114480, DOI: 10.1016/j.addr.2022.114480.

31 X. Ma, N. Gong, L. Zhong, J. Sun and X.-J. Liang, *Biomaterials*, 2016, **97**, 10–21, DOI: 10.1016/j.biomaterials.2016.04.026.

32 G. Bononi, S. Masoni, V. Di Bussolo, T. Tuccinardi, C. Granchi and F. Minutolo, *Semin. Cancer Biol.*, 2022, **86**, 325–333, DOI: 10.1016/j.semcancer.2022.07.003.

33 M. V. Liberti and J. W. Locasale, *Trends Biochem. Sci.*, 2016, **41**, 211–218, DOI: 10.1016/j.tibs.2015.12.001.

34 K. Tilekar, N. Upadhyay, C. V. Iancu, V. Pokrovsky, J.-Y. Choe and C. S. Ramaa, *Biochim. Biophys. Acta, Rev. Cancer*, 2020, **1874**, 188457, DOI: 10.1016/j.bbcan.2020.188457.

35 W. Voigt, *Curr. Opin. Oncol.*, 2018, **30**, 77–83, DOI: 10.1097/cco.0000000000000430.

36 H. W. Kwon, A.-K. Becker, J. M. Goo and G. J. Cheon, *Nucl. Med. Mol. Imaging*, 2017, **51**, 22–31, DOI: 10.1007/s13139-016-0411-3.

37 K. Adekola, S. T. Rosen and M. Shanmugam, *Curr. Opin. Oncol.*, 2012, **24**, 650–654, DOI: 10.1097/cco.0b013e328356da72.

38 L. Szablewski, *Biochim. Biophys. Acta*, 2013, **1835**, 164–169, DOI: 10.1016/j.bbcan.2012.12.004.

39 E. C. Calvaresi and P. J. Hergenrother, *Chem. Sci.*, 2013, **4**, 2319–2333, DOI: 10.1039/c3sc22205e.

40 Y. Anraku, H. Kuwahara, Y. Fukusato, A. Mizoguchi, T. Ishii, K. Nitta, Y. Matsumoto, K. Toh, K. Miyata, S. Uchida, K. Nishina, K. Osada, K. Itaka, N. Nishiyama, H. Mizusawa, T. Yamasoba, T. Yokota and K. Kataoka, *Nat. Commun.*, 2017, **8**, 1001, DOI: 10.1038/s41467-017-00952-3.

41 M. Ismail, J. Liu, N. Wang, D. Zhang, C. Qin, B. Shi and M. Zhen, *Biomaterials*, 2025, **318**, 123138, DOI: 10.1016/j.biomaterials.2025.123138.

42 H.-J. Liu and P. Xu, *Adv. Drug Delivery Rev.*, 2022, **191**, 114619, DOI: 10.1016/j.addr.2022.114619.

43 S. Quader, K. Kataoka and H. Cabral, *Adv. Drug Delivery Rev.*, 2022, **182**, 114115, DOI: 10.1016/j.addr.2022.114115.

44 J. Liu, Y. Cui, H. Cabral, A. Tong, Q. Yue, L. Zhao, X. Sun and P. Mi, *ACS Nano*, 2024, **18**, 25826–25840, DOI: 10.1021/acsnano.4c09053.

45 J. Fu, J. Yang, P. H. Seeberger and J. Yin, *Carbohydr. Res.*, 2020, **498**, 108195, DOI: 10.1016/j.carres.2020.108195.

46 S. S. Mullapudi, D. Mitra, M. Li, E.-T. Kang, E. Chiong and K. G. Neoh, *Mol. Syst. Des. Eng.*, 2020, **5**, 772–791, DOI: 10.1039/c9me00175a.

47 M. Tanasova and J. R. Fedie, *ChemBioChem*, 2017, **18**, 1774–1788, DOI: 10.1002/cbic.201700221.

48 G. Pastuch-Gawolek, J. Szreder, M. Dominska, M. Pielok, P. Cichy and M. Grymel, *Pharmaceutics*, 2023, **15**, 913, DOI: 10.3390/pharmaceutics15030913.

49 D. Drew, R. A. North, K. Nagarathinam and M. Tanabe, *Chem. Rev.*, 2021, **121**, 5289–5335, DOI: 10.1021/acs.chemrev.0c00983.

50 N. Yan, *J. Mol. Biol.*, 2017, **429**, 2710–2725, DOI: 10.1016/j.jmb.2017.07.009.

51 D. Deng, C. Xu, P. Sun, J. Wu, C. Yan, M. Hu and N. Yan, *Nature*, 2014, **510**, 121–125, DOI: 10.1038/nature13306.

52 D. Deng, P. Sun, C. Yan, M. Ke, X. Jiang, L. Xiong, W. Ren, K. Hirata, M. Yamamoto, S. Fan and N. Yan, *Nature*, 2015, **526**, 391–396, DOI: 10.1038/nature14655.

53 K. Kapoor, J. S. Finer-Moore, B. P. Pedersen, L. Caboni, A. Waight, R. C. Hillig, P. Bringmann, I. Heisler, T. Müller, H. Siebeneicher and R. M. Stroud, *Proc. Natl. Acad. Sci. U. S. A.*, 2016, **113**, 4711–4716, DOI: 10.1073/pnas.1603735113.

54 S. Mohan, A. Sheena, N. Poulose and G. Anilkumar, *PLoS One*, 2010, **5**, e14217, DOI: 10.1371/journal.pone.0014217.

55 M.-S. Park, *PLoS One*, 2015, **10**, e0125361, DOI: 10.1371/journal.pone.0125361.

56 C. H. Wu, L.-S. L. Yeh, H. Huang, L. Arminski, J. Castro-Alvear, Y. Chen, Z. Hu, P. Kourtesis, R. S. Ledley, B. E. Suzek, C. R. Vinayaka, J. Zhang and W. C. Barker, *Nucleic Acids Res.*, 2003, **31**, 345–347, DOI: 10.1093/nar/gkg040.

57 Y. Yuan, F. Kong, H. Xu, A. Zhu, N. Yan and C. Yan, *Nat. Commun.*, 2022, **13**, 2671, DOI: 10.1038/s41467-022-30235-5.

58 T. Galochkina, M. N. F. Chong, L. Challali, S. Abbar and C. Etchebest, *Sci. Rep.*, 2019, **9**, 998, DOI: 10.1038/s41598-018-37367-z.

59 S. Gonzalez-Resines, P. J. Quinn, R. J. Naftalin and C. Domene, *J. Chem. Inf. Model.*, 2021, **61**, 3559–3570, DOI: 10.1021/acs.jcim.1c00310.

60 W. Humphrey, A. Dalke and K. Schulten, *J. Mol. Graphics*, 1996, **14**, 33–38, DOI: 10.1016/0263-7855(96)00018-5.

61 X. Fu, G. Zhang, R. Liu, J. Wei, D. Zhang-Negrerie, X. Jian and Q. Gao, *J. Chem. Inf. Model.*, 2016, **56**, 517–526, DOI: 10.1021/acs.jcim.5b00597.

62 H. Liang, A. K. Bourdon, L. Y. Chen, C. F. Phelix and G. Perry, *ACS Chem. Neurosci.*, 2018, **9**, 2815–2823, DOI: 10.1021/acschemneuro.8b00223.

63 Y. Pan, Y. Zhang, P. Gongpan, Q. Zhang, S. Huang, B. Wang, B. Xu, Y. Shan, W. Xiong, G. Li and H. Wang, *Nanoscale Horiz.*, 2018, **3**, 517–524, DOI: 10.1039/c8nh00056e.

64 N. D. Donahue, H. Acar and S. Wilhelm, *Adv. Drug Delivery Rev.*, 2019, **143**, 68–96, DOI: 10.1016/j.addr.2019.04.008.

65 L. A. Dykman and N. G. Khlebtsov, *Chem. Rev.*, 2014, **114**, 1258–1288, DOI: 10.1021/cr300441a.

66 S. Behzadi, V. Serpooshan, W. Tao, M. A. Hamaly, M. Y. Alkawareek, E. C. Dreaden, D. Brown, A. M. Alkilany, O. C. Farokhzad and M. Mahmoud, *Chem. Soc. Rev.*, 2017, **46**, 4218–4244, DOI: 10.1039/c6cs00636a.

67 B. D. Chithrani, J. Stewart, C. Allen and D. A. Jaffray, *Nanomedicine*, 2009, **5**, 118–127, DOI: 10.1016/j.nano.2009.01.008.

68 Z. Krpetic, P. Nativo, V. See, I. A. Prior, M. Brust and M. Volk, *Nano Lett.*, 2010, **10**, 4549–4554, DOI: 10.1021/nl103142t.

69 B. D. Grant and J. G. Donaldson, *Nat. Rev. Mol. Cell Biol.*, 2009, **10**, 597–608, DOI: 10.1038/nrm2755.

70 D. Leto and A. R. Saltiel, *Nat. Rev. Mol. Cell Biol.*, 2012, **13**, 383–396, DOI: 10.1038/nrm3351.

71 K. E. Hamilton, M. F. Bouwer, L. L. Louters and B. D. Looyenga, *Biochimie*, 2021, **190**, 1–11, DOI: 10.1016/j.biochi.2021.06.017.

4898 | *J. Mater. Chem. B*, 2026, **14**, 4874–4902

This journal is © The Royal Society of Chemistry 2026

72 C. C. Barron, P. J. Bilan, T. Tsakiridis and E. Tsiani, *Metabolism*, 2016, **65**, 124–139, DOI: 10.1016/j.metabol. 2015.10.007.

73 J. Ramos-Soriano, M. Ghirardello and M. C. Galan, *Chem. Soc. Rev.*, 2022, **51**, 9960–9985, DOI: 10.1039/d2cs00741j.

74 R. Swami, S. Vij and S. Sharma, *Nanomedicine*, 2024, **19**, 431–453, DOI: 10.2217/nnm-2023-0276.

75 J. E. G. Barnett, G. D. Holman and K. A. Munday, *Biochem. J.*, 1973, **131**, 211–221, DOI: 10.1042/bj1310211.

76 J. Cao, S. Cui, S. Li, C. Du, J. Tian, S. Wan, Z. Qian, Y. Gu, W. R. Chen and G. Wang, *Cancer Res.*, 2013, **73**, 1362–1373, DOI: 10.1158/0008-5472.can-12-2072.

77 T. Halmos, M. Santarromana, K. Antonakis and D. Scherman, *Eur. J. Pharmacol.*, 1996, **318**, 477–484, DOI: 10.1016/s0014-2999(96)00796-0.

78 M. Motiei, T. Dreifuss, O. Betzer, H. Panet, A. Popovtzer, J. Santana, G. Abourbeh, E. Mishani and R. Popovtzer, *ACS Nano*, 2016, **10**, 3469–3477, DOI: 10.1021/acsnano.5b07576.

79 M. Patra, S. G. Awuah and S. J. Lippard, *J. Am. Chem. Soc.*, 2016, **138**, 12541–12551, DOI: 10.1021/jacs.6b06937.

80 J. K. Elter, S. Quader, J. Eichhorn, M. Gottschaldt, K. Kataoka and F. H. Schacher, *Biomacromolecules*, 2021, **22**, 1458–1471, DOI: 10.1021/acs.biomac.0c01661.

81 M. Gynther, J. Ropponen, K. Laine, J. Leppänen, P. Haapakoski, L. Peura, T. Järvinen and J. Rautio, *J. Med. Chem.*, 2009, **52**, 3348–3353, DOI: 10.1021/jm8015409.

82 M. Tanasova, M. Plutschak, M. E. Muroski, S. J. Sturla, G. F. Strouse and D. T. McQuade, *ChemBioChem*, 2013, **14**, 1263–1270, DOI: 10.1002/cbic.201300164.

83 M. S. Hensley, D. Hutchings, A. Ismail and M. Tanasova, *RSC Chem. Biol.*, 2025, **6**, 987–995, DOI: 10.1039/d4cb00239c.

84 M. S. Hensley, A. Oronova, N. Gora, M. R. Geborkoff, N. R. Ostlund, D. R. Fritz, T. Werner and M. Tanasova, *Chem. Biomed. Imaging*, 2023, **1**, 637–647, DOI: 10.1021/cbmi.3c00063.

85 V. V. Begoyan, L. J. Weselinsky, S. Xia, J. Fedie, S. Kannan, A. Ferrier, S. Rao and M. Tanasova, *Chem. Commun.*, 2018, **54**, 3855–3858, DOI: 10.1039/c7cc09809j.

86 N. Nahrjou, A. Ghosh and M. Tanasova, *Int. J. Mol. Sci.*, 2021, **22**, 5073, DOI: 10.3390/ijms22105073.

87 E. C. Cho, J. Xie, P. A. Wurm and Y. Xia, *Nano Lett.*, 2009, **9**, 1080–1084, DOI: 10.1021/nl803487r.

88 T. Dreifuss, T.-S. Ben-Gal, K. Shamalov, A. Weiss, A. Jacob, T. Sadan, M. Motiei and R. Popovtzer, *Nanomedicine*, 2018, **13**, 1535–1549, DOI: 10.2217/nnm-2018-0022.

89 M. Haddad, A. N. Frickenstein and S. Wilhelm, *TrAC, Trends Anal. Chem.*, 2023, **166**, 117172, DOI: 10.1016/j.trac.2023.117172.

90 J.-H. Park, H.-J. Cho and D.-D. Kim, *Int. J. Nanomed.*, 2017, **12**, 7453–7467, DOI: 10.2147/ijn.s147668.

91 C. Douvris, T. Vaughan, D. Bussan, G. Bartzas and R. Thomas, *Sci. Total Environ.*, 2023, **905**, 167242, DOI: 10.1016/j.scitotenv.2023.167242.

92 M. Theerasilp, P. Sunintaboon, W. Sungkarat and N. Nasongkla, *Appl. Nanosci.*, 2017, **7**, 711–721, DOI: 10.1007/s13204-017-0610-y.

93 M. H. Stenzel, *Macromolecules*, 2022, **55**, 4867–4890, DOI: 10.1021/acs.macromol.2c00557.

94 A. Verma and F. Stellacci, *Small*, 2010, **6**, 12–21, DOI: 10.1002/smll.200901158.

95 C. D. Walkey and W. C. W. Chan, *Chem. Soc. Rev.*, 2012, **41**, 2780–2799, DOI: 10.1039/C1CS15233E.

96 H. Nishimura, F. V. Pallardo, G. A. Seidner, S. Vannucci, I. A. Simpson and M. J. Birnbaum, *J. Biol. Chem.*, 1993, **268**, 8514–8520.

97 D. Shishmarev, C. Q. Fontenelle, I. Kuprov, B. Linclau and P. W. Kuchel, *Biophys. J.*, 2018, **115**, 1906–1919, DOI: 10.1016/j.bpj.2018.09.030.

98 Y. Zhang, Y. Ren, H. Xu, L. Li, F. Qian, L. Wang, A. Quan, H. Ma, H. Liu and R. Yu, *ACS Appl. Mater. Interfaces*, 2023, **15**, 10356–10370, DOI: 10.1021/acsami.2c19285.

99 M. O. Koobotse, D. Schmidt, J. M. P. Holly and C. M. Perks, *Int. J. Mol. Sci.*, 2020, **21**, 8674, DOI: 10.3390/ijms21228674.

100 Y. Huang and Z.-G. Xiong, *Cell Stress Chaperones*, 2015, **20**, 1–2, DOI: 10.1007/s12192-014-0547-y.

101 Q. Wang, J. Jin, Z. Guo, F. Chen, Y. Qiu, J. Zhu and Y. Shang, *Cell Stress Chaperones*, 2013, **18**, 367–375, DOI: 10.1007/s12192-012-0390-y.

102 M. L. Fiorello, A. T. Treweeke, D. P. Macfarlane and I. L. Megson, *Sci. Rep.*, 2020, **10**, 19547, DOI: 10.1038/s41598-020-76505-4.

103 C. Gupta and K. Tikoo, *J. Mol. Endocrinol.*, 2013, **51**, 119–129, DOI: 10.1530/JME-13-0062.

104 E. L. da Silva, F. P. Mesquita, A. J. de Sousa Portilho, E. C. A. Bezerra, J. P. Daniel, E. S. P. Aranha, S. Farran, M. C. de Vasconcellos, M. E. A. de Moraes, C. A. Moreira-Nunes and R. C. Montenegro, *Toxicol. In Vitro*, 2022, **82**, 105357, DOI: 10.1016/j.tiv.2022.105357.

105 B. G. Cetiner and M. Y. Terzi, *Cytol. Genet.*, 2022, **56**, 66–76, DOI: 10.3103/S0095452722010054.

106 J. Han, L. Zhang, H. Guo, W. Z. Wysham, D. R. Roque, A. K. Willson, X. Sheng, C. Zhou and V. L. Bae-Jump, *Gynecol. Oncol.*, 2015, **138**, 668–675, DOI: 10.1016/j.ygyno.2015.06.036.

107 N. Rana, M. A. Aziz, R. A. T. Serya, D. S. Lasheen, N. Samir, F. Wuest, K. A. M. Abouzid and F. G. West, *ACS Bio Med Chem Au*, 2023, **3**, 51–61, DOI: 10.1021/acsbiomedchemau.2c00056.

108 D. Kraus, J. Reckenbeil, N. Veit, S. Kuerpig, M. Meisenheimer, I. Beier, H. Stark, J. Winter and R. Probstmeier, *Cell. Oncol.*, 2018, **41**, 485–494, DOI: 10.1007/s13402-018-0385-5.

109 Y. Wang, S. Ma, Z. Dai, Z. Rong and J. Liu, *Nanoscale*, 2019, **11**, 16336–16341, DOI: 10.1039/c9nr03821c.

110 H. S. Min, H. J. Kim, M. Naito, S. Ogura, K. Toh, K. Hayashi, B. S. Kim, S. Fukushima, Y. Anraku, K. Miyata and K. Kataoka, *Angew. Chem., Int. Ed.*, 2020, **59**, 8173–8180, DOI: 10.1002/anie.201914751.

111 X. Jiang, H. Xin, Q. Ren, J. Gu, L. Zhu, F. Du, C. Feng, Y. Xie, X. Sha and X. Fang, *Biomaterials*, 2014, **35**, 518–529, DOI: 10.1016/j.biomaterials.2013.09.094.

112 J. Xie, D. Gonzalez-Carter, T. A. Tockary, N. Nakamura, Y. Xue, M. Nakakido, H. Akiba, A. Dirisala, X. Liu, K. Toh, T. Yang, Z. Wang, S. Fukushima, J. Li, S. Quader, K. Tsumoto, T. Yokota, Y. Anraku and K. Kataoka, *ACS*

This journal is © The Royal Society of Chemistry 2026

J. Mater. Chem. B, 2026, **14**, 4874–4902 | **4899**

Nano, 2020, **14**, 6729–6742, DOI: 10.1021/acsnano.9b09991.

113 Y. Yi, H. J. Kim, M. Zhen, P. Mi, M. Naito, B. S. Kim, H. S. Min, K. Hayashi, F. Perche, K. Toh, X. Liu, Y. Mochida, H. Kinoh, H. Cabral, K. Miyata and K. Kataoka, *J. Controlled Release*, 2019, **295**, 268–277, DOI: 10.1016/j.jconrel.2019.01.006.

114 K. Scherlach, D. Boettger, N. Remme and C. Hertweck, *Nat. Prod. Rep.*, 2010, **27**, 869–886, DOI: 10.1039/b903913a.

115 E. M. Kropp, B. J. Oleson, K. A. Broniowska, S. Bhattacharya, A. C. Chadwick, A. R. Diers, Q. Hu, D. Sahoo, N. Hogg, K. R. Boheler, J. A. Corbett and R. L. Gundry, *Stem Cells Transl. Med.*, 2015, **4**, 483–493, DOI: 10.5966/sctm.2014-0163.

116 D. J. Adams, D. Ito, M. G. Rees, B. Seashore-Ludlow, X. Puyang, A. H. Ramos, J. H. Cheah, P. A. Clemons, M. Warmuth, P. Zhu, A. F. Shamji and S. L. Schreiber, *ACS Chem. Biol.*, 2014, **9**, 2247–2254, DOI: 10.1021/cb500347p.

117 C. D. Walkey, J. B. Olsen, H. Guo, A. Emili and W. C. W. Chan, *J. Am. Chem. Soc.*, 2012, **134**, 2139–2147, DOI: 10.1021/ja2084338.

118 J. Li, J. Yu, Q. Fang, Y. Du and X. Zhang, *ChemBioChem*, 2024, **25**, e202400239, DOI: 10.1002/cbic.202400239.

119 K. Suzuki, Y. Miura, Y. Mochida, T. Miyazaki, K. Toh, Y. Anraku, V. Melo, X. Liu, T. Ishii, O. Nagano, H. Saya, H. Cabral and K. Kataoka, *J. Controlled Release*, 2019, **301**, 28–41, DOI: 10.1016/j.jconrel.2019.02.021.

120 Y. Shi, K. A. Katdare, H. Kim, J. C. Rosch, E. H. Neal, S. Vafaie-Partin, J. A. Bauer and E. S. Lippmann, *Sci. Rep.*, 2023, **13**, 21038, DOI: 10.1038/s41598-023-48361-5.

121 Z. Zhou, Y. Li, S. Chen, Z. Xie, Y. Du, Y. Liu, Y. Shi, X. Lin, X. Zeng, H. Zhao and G. Chen, *Cell Commun. Signaling*, 2024, **22**, 303, DOI: 10.1186/s12964-024-01678-8.

122 G. T. Tietjen, L. G. Bracaglia, W. M. Saltzman and J. S. Pober, *Trends Mol. Med.*, 2018, **24**, 598–606, DOI: 10.1016/j.molmed.2018.05.003.

123 X. Zhang, J. Z. Xing, J. Chen, L. Ko, J. Amanie, S. Gulavita, N. Pervez, D. Yee, R. Moore and W. Roa, *Clin. Invest. Med.*, 2008, **31**, E160–E167, DOI: 10.25011/cim.v31i3.3473.

124 W. Roa, X. Zhang, L. Guo, A. Shaw, X. Hu, Y. Xiong, S. Gulavita, S. Patel, X. Sun, J. Chen, R. Moore and J. Z. Xing, *Nanotechnology*, 2009, **20**, 375101, DOI: 10.1088/0957-4484/20/37/375101.

125 F. Geng, K. Song, J. Z. Xing, C. Yuan, S. Yan, Q. Yang, J. Chen and B. Kong, *Nanotechnology*, 2011, **22**, 285101, DOI: 10.1088/0957-4484/22/28/285101.

126 T.-M. Cheng, H.-L. Chu, Y.-C. Lee, D.-Y. Wang, C.-C. Chang, K.-L. Chung, H.-C. Yen, C.-W. Hsiao, X.-Y. Pan, T.-R. Kuo and C.-C. Chen, *Anal. Chem.*, 2018, **90**, 3974–3980, DOI: 10.1021/acs.analchem.7b04961.

127 F. Porcaro, C. Battocchio, A. Antoccia, I. Fratoddi, I. Venditti, A. Fracassi, I. Luisetto, M. V. Russo and G. Polzonetti, *Colloids Surf., B*, 2016, **142**, 408–416, DOI: 10.1016/j.colsurfb.2016.03.016.

128 C. Hu, M. Niestroj, D. Yuan, S. Chang and J. Chen, *Int. J. Nanomed.*, 2015, **10**, 2065–2077, DOI: 10.2147/ijn.s72144.

129 M. Morais, V. Machado, F. Dias, P. Figueiredo, C. Palmeira, G. Martins, R. Fernandes, A. R. Malheiro, K. S. Mikkonen,

A. L. Teixeira and R. Medeiros, *Int. J. Nanomed.*, 2022, **17**, 4321–4337, DOI: 10.2147/ijn.s364862.

130 E. Asik, T. N. Aslan, M. Volkan and N. T. Güray, *Environ. Toxicol. Pharmacol.*, 2016, **41**, 272–278, DOI: 10.1016/j.etap.2015.12.004.

131 P. M. A. de Farias, B. S. Santos, F. D. Menezes, A. G. Brasil Jr., R. Ferreira, M. A. Motta, A. G. Castro-Neto, A. A. S. Vieira, D. C. N. Silva, A. Fontes and C. L. Cesar, *Appl. Phys. A: Mater. Sci. Process.*, 2007, **89**, 957–961, DOI: 10.1007/s00339-007-4267-3.

132 E. Niemelä, D. Desai, Y. Nkizinkiko, J. E. Eriksson and J. M. Rosenholm, *Eur. J. Pharm. Biopharm.*, 2015, **96**, 11–21, DOI: 10.1016/j.ejpb.2015.07.009.

133 C. D. Fahrenholtz, M. Hadimani, S. B. King, S. V. Torti and R. Singh, *Nanomedicine*, 2015, **10**, 2481–2497, DOI: 10.2217/nnm.15.90.

134 A. Lundqvist and P. Lundahl, *J. Chromatogr. A*, 1997, **776**, 87–91, DOI: 10.1016/s0021-9673(97)00029-0.

135 I. Sur, D. Cam, M. Kahraman, A. Baysal and M. Culha, *Nanotechnology*, 2010, **21**, 175104, DOI: 10.1088/0957-4484/21/17/175104.

136 D. C. Kennedy, G. Orts-Gil, C.-H. Lai, L. Miller, A. Haase, A. Luch and P. H. Seeberger, *J. Nanobiotechnol.*, 2014, **12**, 59, DOI: 10.1186/s12951-014-0059-z.

137 J. Salado, M. Insausti, L. Lezama, I. Gil de Muro, M. Moros, B. Pelaz, V. Grazu, J. M. de la Fuente and T. Rojo, *Nanotechnology*, 2012, **23**, 315102, DOI: 10.1016/10.1088/0957-4484/23/31/315102.

138 M. Moros, B. Hernaez, E. Garet, J. T. Dias, B. Saez, V. Grazu, A. Gonzalez-Fernandez, C. Alonso and J. M. de la Fuente, *ACS Nano*, 2012, **6**, 1565–1577, DOI: 10.1021/nn204543c.

139 J. H. Ahire, M. Behray, C. A. Webster, Q. Wang, V. Sherwood, N. Saengkrit, U. Ruktanonchai, N. Woramongkolchai and Y. Chao, *Adv. Healthcare Mater.*, 2015, **4**, 1877–1886, DOI: 10.1002/adhm.201500298.

140 C. Tzror-Azankot, A. Anaki, T. Sadan, M. Motiei and R. Popovtzer, in *Nanoscale Imaging, Sensing, and Actuation for Biomedical Applications XXII*, ed D. Fixler and S. Wachsmann-Hogiu, SPIE, San Francisco, 2025, Vol. 13335. , DOI: 10.1117/12.3044899.

141 C.-W. Hsu, D. Septiadi, C.-H. Lai, P. Chen, P. H. Seeberger and L. De Cola, *ChemPlusChem*, 2017, **82**, 660–667, DOI: 10.1002/cplu.201700054.

142 B. Mehravi, M. Ahmadi, M. Amanlou, A. Mostaar, M. S. Ardestani and N. Ghalandarlaki, *Int. J. Nanomed.*, 2013, **8**, 3383–3394, DOI: 10.2147/ijn.s44829.

143 B. D. Chithrani, A. A. Ghazani and W. C. W. Chan, *Nano Lett.*, 2006, **6**, 662–668, DOI: 10.1021/nl052396o.

144 T. Kanamori, T. Sawamura, T. Tanaka, I. Sotokawa, R. Mori, K. Inada, A. Ohkubo, S.-I. Ogura, Y. Murayama, E. Otsuji and H. Yuasa, *Bioorg. Med. Chem.*, 2017, **25**, 743–749, DOI: 10.1016/j.bmc.2016.11.050.

145 S. K. Basiruddin, A. R. Maity and N. R. Jana, *RSC Adv.*, 2012, **2**, 11915–11921, DOI: 10.1039/c2ra22055e.

146 X.-L. Ge, B. Huang, Z.-L. Zhang, X. Liu, M. He, Z. Yu, B. Hu, R. Cui, X.-J. Liang and D.-W. Pang, *J. Mater. Chem. B*, 2019, **7**, 5782–5788, DOI: 10.1039/c9tb01112a.

4900 | *J. Mater. Chem. B*, 2026, **14**, 4874–4902

This journal is © The Royal Society of Chemistry 2026

147 B. Aydogan, J. Li, T. Rajh, A. Chaudhary, S. J. Chmura, C. Pelizzari, C. Wietholt, M. Kurtoglu and P. Redmond, *Mol. Imaging Biol.*, 2010, **12**, 463–467, DOI: 10.1007/s11307-010-0299-8.

148 T. N. Aslan, E. Asik, N. T. Güray and M. Volkan, *J. Biol. Inorg. Chem.*, 2020, **25**, 1139–1152, DOI: 10.1007/s00775-020-01830-y.

149 A. Mazur, I. Litt and E. Shorr, *J. Biol. Chem.*, 1950, **187**, 473–484, DOI: 10.1016/S0021-9258(18)56191-3.

150 R. R. Rajeshkumar, P. Pavadai, T. Panneerselvam, V. Deepak, S. R. K. Pandian, S. J. Kabilan, S. Vellaichamy, A. Jeyaraman, A. S. K. Kumar, K. Sundar and S. Kunjiappan, *Naunyn-Schmiedeberg's Arch. Pharmacol.*, 2023, **396**, 2571–2586, DOI: 10.1007/s00210-023-02480-y.

151 S. Shen, M. Du, Q. Liu, P. Gao, J. Wang, S. Liu and L. Gu, *Nanoscale*, 2020, **12**, 21901–21912, DOI: 10.1039/d0nr05138a.

152 J. Li, F.-K. Ma, Q.-F. Dang, X.-G. Liang and X.-G. Chen, *Front. Mater. Sci.*, 2014, **8**, 363–372, DOI: 10.1007/s11706-014-0262-8.

153 A. Dag, M. Callari, H. Lu and M. H. Stenzel, *Polym. Chem.*, 2016, **7**, 1031–1036, DOI: 10.1039/c5py01579k.

154 J. S. Basuki, L. Esser, H. T. T. Duong, Q. Zhang, P. Wilson, M. R. Whittaker, D. M. Haddleton, C. Boyer and T. P. Davis, *Chem. Sci.*, 2014, **5**, 715–726, DOI: 10.1039/c3sc52838c.

155 R. Gromnicova, H. A. Davies, P. Sreekanthreddy, I. A. Romero, T. Lund, I. M. Roitt, J. B. Phillips and D. K. Male, *PLoS One*, 2013, **8**, e81043, DOI: 10.1371/journal.pone.0081043.

156 L. Venturelli, S. Nappini, M. Bulfoni, G. Gianfranceschi, S. Dal Zilio, G. Coceano, F. Del Ben, M. Turetta, G. Scoles, L. Vaccari, D. Cesselli and D. Cojoc, *Sci. Rep.*, 2016, **6**, 21629, DOI: 10.1038/srep21629.

157 C. Xintaropoulou, C. Ward, A. Wise, H. Marston, A. Turnbull and S. P. Langdon, *Oncotarget*, 2015, **6**, 25677–25695, DOI: 10.18632/oncotarget.4499.

158 X. H. Shan, H. Hu, F. Xiong, N. Gu, X. D. Geng, W. Zhu, J. Lin and Y. F. Wang, *Eur. J. Radiol.*, 2012, **81**, 95–99, DOI: 10.1016/j.ejrad.2011.03.013.

159 F. Xiong, Z.-y Zhu, C. Xiong, X.-q Hua, X.-h Shan, Y. Zhang and N. Gu, *Pharm. Res.*, 2012, **29**, 1087–1097, DOI: 10.1007/s11095-011-0653-9.

160 X. H. Shan, P. Wang, F. Xiong, N. Gu, H. Hu, W. Qian, H. Y. Lu and Y. Fan, *Mol. Imaging Biol.*, 2016, **18**, 24–33, DOI: 10.1007/s11307-015-0874-0.

161 D. Mumcuoglu, M. S. Ekiz, G. Gunay, T. Tekinay, A. B. Tekinay and M. O. Guler, *ACS Appl. Mater. Interfaces*, 2016, **8**, 11280–11287, DOI: 10.1021/acsami.6b01526.

162 Q. Wang, T. Wang, C. Lio, X. Yu, X. Chen, L. Liu, Y. Wu, H. Huang, L. Qing and P. Luo, *J. Controlled Release*, 2023, **356**, 678–690, DOI: 10.1016/j.jconrel.2023.03.008.

163 H. Shinchi, M. Wakao, S. Nakagawa, E. Mochizuki, S. Kuwabata and Y. Suda, *Chem. - Asian J.*, 2012, **7**, 2678–2682, DOI: 10.1002/asia.201200362.

164 E. S. Seven, S. K. Sharma, D. Meziane, Y. Zhou, K. J. Mintz, R. R. Pandey, C. C. Chusuei and R. M. Leblanc, *Langmuir*, 2019, **35**, 6708–6718, DOI: 10.1021/acs.langmuir.9b00920.

165 E. S. Seven, Y. B. Seven, Y. Zhou, S. Poudel-Sharma, J. J. Diaz-Rucco, E. K. Cilingir, G. S. Mitchell, J. D. Van Dyken and R. M. Leblanc, *Nanoscale Adv.*, 2021, **3**, 3942–3953, DOI: 10.1039/d1na00145k.

166 S. A. Baldwin, *Biochim. Biophys. Acta*, 1993, **1154**, 17–49, DOI: 10.1016/0304-4157(93)90015-G.

167 T.-T. Yu, X.-C. Peng, M.-F. Wang, N. Han, H.-Z. Xu, Q.-R. Li, L.-G. Li, X. Xu, Q.-L. Ma, B. Liu, J. Wang, L. Zhao, X. Chen and T.-F. Li, *J. Cancer Res. Clin. Oncol.*, 2022, **148**, 867–879, DOI: 10.1007/s00432-021-03879-x.

168 V. Mamaeva, R. Niemi, M. Beck, E. Özliseli, D. Desai, S. Landor, T. Gronroos, P. Kronqvist, I. K. N. Pettersen, E. McCormack, J. M. Rosenholm, M. Linden and C. Sahlgren, *Mol. Ther.*, 2016, **24**, 926–936, DOI: 10.1038/mt.2016.42.

169 A. P. P. Kröger, M. I. Komil, N. M. Hamelmann, A. Juan, M. H. Stenzel and J. M. J. Paulusse, *ACS Macro Lett.*, 2019, **8**, 95–101, DOI: 10.1021/acsmacrolett.8b00812.

170 R. S. Dhanikula, A. Argaw, J.-F. Bouchard and P. Hildgen, *Mol. Pharmaceutics*, 2008, **5**, 105–116, DOI: 10.1021/mp700086j.

171 S. A. Torres-Perez, M. del Pilar Ramos-Godinez and E. Ramon-Gallegos, *J. Drug Delivery Sci. Technol.*, 2020, **58**, 101769, DOI: 10.1016/j.jddst.2020.101769.

172 A. S. Taleghani, P. Ebrahimnejad, A. Heidarinasab and A. Akbarzadeh, *Mater. Sci. Eng., C*, 2019, **98**, 358–368, DOI: 10.1016/j.msec.2018.12.138.

173 A. Abolhasani, D. Biria, H. Abolhasani, A. Zarrabi and T. Komeili, *Int. J. Nanomed.*, 2019, **14**, 9535–9546, DOI: 10.2147/ijn.s228652.

174 A. Bukchin, N. Kuplennik, A. M. Carcaboso and A. Sosnik, *Appl. Mater. Today*, 2018, **11**, 57–69, DOI: 10.1016/j.apmt.2018.01.003.

175 A. Bukchin, G. Pascual-Pasto, M. Cuadrado-Vilanova, H. Castillo-Ecija, C. Monterrubio, N. G. Olaciregui, M. Vila-Ubach, L. Ordeix, J. Mora, A. M. Carcaboso and A. Sosnik, *J. Controlled Release*, 2018, **276**, 59–71, DOI: 10.1016/j.jconrel.2018.02.034.

176 N. Lecot, R. Glisoni, N. Oddone, J. Benech, M. Fernández, J. P. Gambini, P. Cabral and A. Sosnik, *Adv. Ther.*, 2021, **4**, 2000010, DOI: 10.1002/smll.20070079410.1002/adtp.202000010.

177 I. Zlotver and A. Sosnik, *Small*, 2024, **20**, 2305475, DOI: 10.1002/smll.202305475.

178 M. Theerasilp, P. Chalermpanapun, P. Sunintaboon, W. Sungkarat and N. Nasongkla, *J. Mater. Sci.: Mater. Med.*, 2018, **29**, 177, DOI: 10.1007/s10856-018-6177-7.

179 M. A. Moretton, E. Bernabeu, E. Grotz, L. Gonzalez, M. Zubillaga and D. A. Chiappetta, *Eur. J. Pharm. Biopharm.*, 2017, **114**, 305–316, DOI: 10.1016/j.ejpb.2017.02.005.

180 J. K. Elter, F. Sedlak, T. Palusak, N. Bernardova, V. Lobaz, E. Tihlarikova, V. Nedela, P. Sacha and M. Hruby, *Biomacromolecules*, 2025, **26**, 861–882, DOI: 10.1021/acs.biomac.4c01052.

181 H. Wang, X. Wang, C. Xie, M. Zhang, H. Ruan, W. Songli, K. Jiang, F. Wang, C. Zhan, W. Lu and H. Wang, *J. Controlled Release*, 2018, **284**, 26–38, DOI: 10.1016/j.jconrel.2018.06.006.

This journal is © The Royal Society of Chemistry 2026

J. Mater. Chem. B, 2026, **14**, 4874–4902 | **4901**

182 Q. Jin, L. Agrawal, Z. VanHorn-Ali and G. Alkhatib, *Virology*, 2006, **353**, 99–110, DOI: 10.1016/j.virol.2006.05.003.

183 H. Wang, Z. Zhang, J. Guan, W. Lu and C. Zhan, *Asian J. Pharm. Sci.*, 2021, **16**, 120–128, DOI: 10.1016/j.ajps.2020.07.001.

184 M. Brownlee, *Nature*, 2001, **414**, 813–820, DOI: 10.1038/414813a.

185 Q. Fu, Y. Zhao, Z. Yang, Q. Yue, W. Xiao, Y. Chen, Y. Yang, L. Guo and Y. Wu, *Arch. Pharm.*, 2019, **352**, 1800219, DOI: 10.1002/ardp.201800219.

186 Q. Liu, L. Zhou, R. Lu, C. Yang, S. Wang, L. Hai and Y. Wu, *Bioorg. Med. Chem.*, 2021, **29**, 115852, DOI: 10.1016/j.bmc.2020.115852.

187 F. Xie, N. Yao, Y. Qin, Q. Zhang, H. Chen, M. Yuan, J. Tang, X. Li, W. Fan, Q. Zhang, Y. Wu, L. Hai and Q. He, *Int. J. Nanomed.*, 2012, **7**, 163–175, DOI: 10.2147/ijn.s23771.

188 Y. Zhang, H. Qu and X. Xue, *Biomater. Sci.*, 2022, **10**, 423–434, DOI: 10.1039/d1bm01506k.

189 Q. Duan, R. Liu, J.-Q. Luo, J.-Y. Zhang, Y. Zhou, J. Zhao and J.-Z. Du, *Nano Lett.*, 2024, **24**, 402–410, DOI: 10.1021/acs.nanolett.3c04175.

190 O. Betzer, N. Perets, A. Angel, M. Motiei, T. Sadan, G. Yadid, D. Offen and R. Popovtzer, *ACS Nano*, 2017, **11**, 10883–10893, DOI: 10.1021/acsnano.7b04495.

191 H. Y. Zhu, S. Y. Zhang, Y. Ling, G. L. Meng, Y. Yang and W. Zhang, *J. Controlled Release*, 2015, **220**, 529–544, DOI: 10.1016/j.jconrel.2015.11.017.

192 Y.-C. Yeh, S. T. Kim, R. Tang, B. Yan and V. M. Rotello, *J. Mater. Chem. B*, 2014, **2**, 4610–4614, DOI: 10.1039/c4tb00608a.

193 K. S. Sharma, P. K. Melwani, H. D. Yadav, R. Joshi, N. G. Shetake, A. K. Dubey, B. P. Singh, S. Phapale, P. P. Phadnis, R. K. Vatsa, R. S. Ningthoujam and B. N. Pandey, *RSC Adv.*, 2023, **13**, 13240–13251, DOI: 10.1039/d3ra01169k.

194 P. Ma, J. Chen, X. Bi, Z. Li, X. Gao, H. Li, H. Zhu, Y. Huang, J. Qi and Y. Zhang, *ACS Appl. Mater. Interfaces*, 2018, **10**, 12351–12363, DOI: 10.1021/acsami.7b18437.

195 P. Ma, Y. Sun, J. Chen, H. Li, H. Zhu, X. Gao, X. Bi and Y. Zhang, *Drug Delivery*, 2018, **25**, 153–165, DOI: 10.1080/10717544.2017.1419511.

196 K. Sztandera, P. Dzialak, M. Marcinkowska, M. Stanczyk, M. Gorzkiewicz, A. Janaszewska and B. Klajnert-Maculewicz, *Pharm. Res.*, 2019, **36**, 140, DOI: 10.1007/s11095-019-2673-9.

197 J. Hadar, S. Skidmore, J. Garner, H. Park, K. Park, Y. Wang, B. Qin and X. Jiang, *J. Controlled Release*, 2019, **304**, 75–89, DOI: 10.1016/j.jconrel.2019.04.039.

198 X. Jiang, H. Xin, J. Gu, F. Du, C. Feng, Y. Xie and X. Fang, *J. Pharm. Sci.*, 2014, **103**, 1487–1496, DOI: 10.1002/jps.23928.

199 Y. Li, W. Hong, H. Zhang, T. T. Zhang, Z. Chen, S. Yuan, P. Peng, M. Xiao and L. Xu, *J. Controlled Release*, 2020, **317**, 232–245, DOI: 10.1016/j.jconrel.2019.11.031.

200 J. Niu, A. Wang, Z. Ke and Z. Zheng, *J. Drug Targeting*, 2014, **22**, 712–723, DOI: 10.3109/1061186X.2014.913052.

201 C.-X. Zhang, W.-Y. Zhao, L. Liu, R.-J. Ju, L.-M. Mu, Y. Zhao, F. Zeng, H.-J. Xie, Y. Yan and W.-L. Lu, *Oncotarget*, 2015, **6**, 32681–32700, DOI: 10.18632/oncotarget.5354.

202 D. Liu, Y. Cheng, S. Qiao, M. Liu, Q. Ji, B.-L. Zhang, Q.-B. Mei and S. Zhou, *ACS Nano*, 2022, **16**, 7409–7427, DOI: 10.1021/acsnano.1c09794.

203 Y. Zhu, J. Liang, C. Gao, A. Wang, J. Xia, C. Hong, Z. Zhong, Z. Zuo, J. Kim, H. Ren, S. Li, Q. Wang, F. Zhang and J. Wang, *J. Controlled Release*, 2021, **330**, 641–657, DOI: 10.1016/j.jconrel.2020.12.036.

204 C. Tzror-Azankot, O. Betzer, T. Sadan, M. Motiei, S. Rahimipour, A. Atkins, A. Popovtzer and R. Popovtzer, *ACS Nano*, 2021, **15**, 1301–1309, DOI: 10.1021/acsnano.0c08530.

205 H. Hinterwirth, S. Kappel, T. Waitz, T. Prohaska, W. Lindner and M. Lämmerhofer, *ACS Nano*, 2013, **7**, 1129–1136, DOI: 10.1021/nn306024a.

206 B. S. Purohit, A. Ailianou, N. Dulguerov, C. D. Becker, O. Ratib and M. Becker, *Insights Imaging*, 2014, **5**, 585–602, DOI: 10.1007/s13244-014-0349-x.

4902 | *J. Mater. Chem. B*, 2026, **14**, 4874–4902

This journal is © The Royal Society of Chemistry 2026